Negative ion source operation with deuterium

M. Bacal, M Wada

Plasma Sources Science and Technology

TOPICAL REVIEW • OPEN ACCESS

Negative ion source operation with deuterium

OPEN ACCESS
IOP Publishing
Plasma Sources Science and Technology
Plasma Sources Sci. Technol. **29** (2020) 033001 (22pp)
https://doi.org/10.1088/1361-6595/ab6881

Topical Review

Negative ion source operation with deuterium

M Bacal[1,3] **and M Wada**[2]

[1] UPMC, Ecole Polytechnique, LPP, UMR CNRS 7648, Palaiseau, France
[2] School of Science and Engineering, Doshisha University, Kyotanabe, Kyoto 610-0321, Japan

E-mail: marthabacal@orange.fr and mwada@mail.doshisha.ac.jp

Received 25 October 2019, revised 13 December 2019
Accepted for publication 7 January 2020
Published 4 March 2020

Abstract

When the working gas of a negative ion source is changed from hydrogen to its isotope, deuterium, an 'isotope effect' is observed; namely, several plasma characteristics such as the electron energy distribution, the atomic fraction and the spectra of rovibrationally excited molecules change. The understanding of the effect becomes more important, as research and development aiming at ITER power level operation is being challenged with feeding deuterium to the ion sources. As a historical review of the effort to develop hydrogen/deuterium negative ion sources, several types of negative ion sources designed for the neutral beam plasma heating are described: double charge exchange sources, volume sources and surface-plasma sources. The early results with volume sources operated with and without cesium are introduced. The characteristics of the source charged with deuterium are compared to those of the source charged with hydrogen. The isotope effect did not appear pronounced as the negative ion density was measured in a small source but became more pronounced when the plasma source size was enlarged and the discharge power density was increased to higher values. Surface plasma sources were optimized for deuterium operation but could not achieve the same performance as a source operated with hydrogen at the same power and pressure. The lower velocity of negative deuterium ions leaving the low work function surface seemed to limit the production efficiency. Fundamental processes causing these differences in negative ion source operation are summarized. After explaining the current status of negative ion source research and development, the acquired knowledge is utilized to the development of large negative ion sources for nuclear fusion research and to the development of compact negative ion sources for neutron source applications.

Keywords: negative ions, hydrogen, deuterium, charge exchange, volume negative ion sources, surface negative ion sources

Introduction

The nuclear fusion reaction occurs in the collision of a deuterium atom with a tritium atom (D–T reaction), leading to the formation of a helium atom and a neutron. The fusion reaction occurs also in the collision of two deuterium atoms (D–D reaction), but the cross section for the D–D fusion reaction in the energy range 20–100 keV is two orders of magnitude less than that for the D–T reaction [1]. The thermonuclear fusion reaction is a way to achieve nuclear fusion by using extremely high temperatures. Magnetic confinement fusion is an approach to generate thermonuclear fusion power that uses magnetic fields to confine the hot fusion fuel in the form of plasma. In 1950s Igor Tamm and Andrei Sakharov invented the tokamak magnetic confinement device. The first tokamak

[3] Author to whom any correspondence should be addressed.

named T1 was built at Kurchatov Institute in Moscow. Since then, the magnetic fusion research field has been dominated by the tokamak approach.

The international collaboration fusion project ITER is now in its construction phase and designs of all components including the plasma heating and fuel breeding systems have been fixed already. However, several problems are still unresolved [2] and the ITER project will provide physics data for the engineering as well as scientific background of the DEMO reactor. The fusion reactor DEMO should be the first power plant that proves the economical generation of electricity from nuclear fusion [3]. This means that all the components constituting a fusion reactor can be improved further from the ITER design to make DEMO more efficient than ITER. For example, a more efficient method of producing neutral deuterium beams for DEMO by photodetachment is investigated [4]. Many other projects develop in the world, including the Broader Approach agreement to ITER [5]:

- a medium size tokamak, T-15MD is under construction at Kurchatov Institute in Moscow, Russia [6]
- a spherical tokamak GLOBUS-M2 is under construction at Ioffe Physical-Technical Institute in St. Petersbourg, Russia [7]
- the Australian Plasma Fusion Research Facility (APFRF) upgraded the H-1Heliac, a large stellarator device located at ANU (Australian National University) in Canberra, called H-1NF [8] and research is conducted for producing negative ion beams using a high-power helicon discharge source [9].
- The Broader Approach agreement, concluded between the European Atomic Energy Community (Euratom) and Japan, consists of activities which aim to complement the ITER project and to accelerate the realization of fusion energy through R&D and advanced technologies for future demonstration of fusion power reactors (DEMO).

The JT-60SA (SA = Super Advanced) is a fusion experiment designed to support the operation of ITER and to investigate how to optimize the operation of fusion power plants that will be built after ITER [10]. It is a joint international research and development project involving Japan and Europe, and is to be built in Naka (Japan) using the infrastructure of the former generation JT-60.

An overview of Japanese fusion engineering research activities focusing on those being carried out by the National Institute for Fusion Science (NIFS) and Japanese universities (Universities) is given by Muroga *et al* [11]. NIFS is promoting the Fusion Engineering Research Project (FERP) as one of three research projects. The majority of the activity in FERP is being carried out by collaboration with Universities. Utilizing the core facilities installed in NIFS and the unique infrastructures of Universities, collaboration between NIFS and Universities is performed for the superconducting magnet, the liquid breeder blanket, advanced materials, high heat flux components, and tritium safety. NIFS also carries out international collaboration programs such as Japan–China-based, Japan–US-based, and International Energy Agency-based collaborations, promoting participation of University researchers. Division of responsibilities with the National Institutes for Quantum and Radiological Science and Technology (QRST), contributions to the ITER Broader Approach, and the Action Plan Toward DEMO Development are also reported.

The magnetic fields which prevent the escape of plasma from a tokamak fusion reactor preclude the direct injection of charged particles. Therefore, it is necessary to inject deuterium and tritium, the reacting species in the favored D–T reaction, as 'neutral atoms'. If these neutrals are injected with sufficient energy, they can heat the confined plasma up to the about 10 keV temperature required to produce a self-sustained fusion reaction. Energetic neutral beams can be made from either positive ion beams or negative ion beams. The necessary neutralizer target thickness to convert energetic ion beams to neutral beams rises with energy; at an energy below about 20 keV for H^+ ions the effective thickness of the charge transfer target can always be made large enough to realize a virtually 100% efficiency to convert positive ions to neutral beams. For higher energies the decrease in charge transfer cross section cannot be overcome by an increase in the thickness of the charge transfer target to achieve a nearly complete conversion to neutrals, because of a competition with the re-ionization. For H^+ beams of more than 100 keV and D^+ beams of more than 200 keV to make the neutral beams reach the core plasma region, the efficiency for converting ions to neutrals is falling so rapidly with energy that it is not feasible to use positive ion beams for the generation of neutrals at these higher energies.

The generation of neutral beams by the stripping of the outermost electron from the negative ion is not subject to any high energy limitation. The competitive process in this case is also the ionization of the neutral, but the ratio of the cross sections for the reactions $D^- \rightarrow D^\circ$ and $D^\circ \rightarrow D^+$ is independent of energy at high energy. The importance of negative ion based neutral beam injection (NBI) systems for future fusion devices became obvious in the early 1970s. Berkner *et al* [12] reported that the acceleration of D^- ion beam was the only possible way to achieve efficient neutral-beam injection into fusion devices with the beam energy exceeding 100 keV per nucleon. High neutralization efficiencies can be achieved for accelerated negative ion beams using a gas neutralizer (approximately 60%), a plasma neutralizer (<80%), or a photon neutralizer (up to 100%). A gas neutralizer cell of the correct thickness is capable, according to Fink and Hamilton [13] of yielding 60%–65% neutrals from an incident D^- beam, independent of energy. It was thus concluded from the above discussion that, with the enhancement of the energy required for the neutral beams, the activity of the NBI development had to move from positive ion injection to negative ion injection. Obviously, the system has to provide not only hydrogen neutral beams, but also enough performance to generate deuterium and tritium neutral beams for successful fusion reaction.

An important step in the European R&D roadmap of the NBI systems for ITER is the successful operation of negative ion source test facility ELISE [2] (Extraction from Large Ion Source Experiment). Its aim is to better understand the open

physics issues related to the source size extrapolation from the prototype RF source ($0.3 \times 0.6\,m^2$) to the full ITER size ($0.9 \times 2.0\,m^2$) [14]. The main challenges to be met are:

- the amount and temporal stability of co-extracted electrons, especially in deuterium operation [14–20] since the co-extracted electron current has to remain below the extracted negative ion current for technological reasons (in order to avoid the excessive heat loading to the extraction grid),
- the caesium management [21] since the choice of a caesium injection type ion source for ITER implies, at least on the first stage, the use of caesium vapor for reducing the work function of one of the electrodes,
- finding low work function materials that can ensure the caesium-free negative ion source operation [2].

Due to safety regulations, experiments accelerating D^- were not frequent as they produce neutrons and tritons. Accelerated deuterons are implanted at the beam strike point and react with beam deuterons. Note that neutron generation does not take place during beam acceleration. Recently, D^- ion sources have been used to produce D° (neutral deuterium) beams for injecting energy into deuterium plasmas, as it is necessary to design a future fusion experiment system with high energy fuel beams ($\gg$100 keV/nucleon) and to understand deeper the proper plasma operation of the confinement device under an intense background radiation condition [22]. However, the sources being developed in view of the ITER plasma heating often exhibit poor performance when the gas in the ion source is replaced from hydrogen to deuterium [23]. Research and development of negative ion based neutral beam heating systems is directed towards long pulse operation of large, ITER size sources with deuterium [24]. Simonin *et al* [4] and Fantz *et al* [2] describe the research and development efforts dedicated in Europe to the NBI for the tokamak DEMO. In Japan the superconductor helical system, Large Helical Device (LHD) at National Institute for Fusion Science, is now investigating deuterium plasmas with negative ion based neutral beam heating charged with deuterium [25]. A negative ion source cannot produce negative deuterium (D^-) ion current as large as the negative hydrogen (H^-) ion current using identical parameters, e.g. using the same power. The sources require more Cs to produce enough D^- beam current, while improvements are necessary to reduce co-extracted electron current [15, 16]. The improvements are [16]:

- installing in front of the first grid a stronger magnetic filter field, generated by a current of several kA flowing through the grid, and applying a higher bias to it.
- installing additional permanent magnets attached to the lateral sides of the source.
- applying refined Cs evaporation and distribution procedures.

The plasma density in deuterium is in general higher than in hydrogen at the same parameters [17, 18, 20]. This is seen as the reason for the higher current of co-extracted electrons compared to hydrogen operation. Different target parameters for the SPIDER (Source for Production of Ion of Deuterium Extracted from an RF plasma) device, the full-size prototype of the negative ion source and extractor for the ITER Heating Neutral Beam, were set for hydrogen and deuterium: 355 A m^{-2} H^- current density against 285 A m^{-2} D^- current density, and 0.5 electron current fraction for H^- as compared to 1.0 electron current fraction for D^- beam current [26]. The SPIDER device has started the first operation phase in June 2018 to fulfill the requirements from ITER, while the ELISE project with the size one half of the SPIDER demonstrated 230 A m^{-2} accelerated H^- current density for more than 1000 s, which is the ITER requirement [27]. The challenges for D^- beam extraction with these ITER size large machines have begun.

The comparison between the source performance when operated with hydrogen and that with deuterium was investigated from early days without Cs injection using arc discharge sources [28–30] instead of advanced RF sources to be installed in ITER [31]. Based on the above background of nuclear fusion research and development, this article briefly summarizes the physical reasons for observing the difference in ion source performance between hydrogen and deuterium, the two hydrogen isotopes. Then the article presents the history of the development of the hydrogen and deuterium negative ion sources; the first negative ion sources were the charge exchange negative ion sources. They were followed by the volume negative ion sources in pure hydrogen or deuterium, and in hydrogen or deuterium with caesium injection, in which the main production mechanism of H^-/D^- is the dissociative electron attachment to hydrogen/deuterium molecules. Next, the surface production ion sources are presented, in which the dominant production mechanism is the negative surface ionization of the incident particles on the surfaces. Two general features of the volume and surface negative ion sources are:

(1) The presence of a magnetic filter, producing a magnetic field which separates the source into two regions: the driver, where fast electrons ionize the gas, and the extraction region, characterized by a low electron temperature, where negative ions are formed.
(2) The presence of an electrically biased plasma electrode containing an extraction opening. This electrode separates the ion source extraction region from the extraction and acceleration structure; it is also called 'a plasma grid' when beams are extracted through multi-apertures opened on this electrode. The roles of the plasma grid in negative ion sources [32] are: optimizing the extracted negative ion current, reducing the co-extracted electron current, controlling the axial plasma potential profile, recycling the hydrogen or deuterium atoms to molecules, concentrating the negative ions near its surface. A function specific for surface production ion sources is the direct emission of negative ions under positive ion and neutral hydrogen or deuterium bombardment.

Since ion sources for direct neutron production applications are operated with deuterium [1, 33], this article also covers topics on neutron production as an application of the source operation physics.

Production and destruction processes of negative hydrogen isotope ions

Two mechanisms of producing H^-/D^- ions are discussed: production in the plasma volume and on the surface facing the plasma. The difference between the behavior of ion sources operating in deuterium and that of ion sources operating in hydrogen will be pointed out.

Negative ion production and destruction processes in the plasma volume

Depending upon the reaction process, hydrogen and deuterium have different cross sections because of several reasons. Firstly, the reduced masses of H_2 and D_2 systems are different, causing their vibrational and rotational levels to be different. Secondly, a deuteron is a spin 1 boson, while a proton is a fermion with the spin $1/2$. Thus, plasmas of hydrogen and deuterium can be similar due to the electronic configurations of their ions but they should show differences according to the nuclear configurations of their ions. The main physical reason for observing different cross sections for the same reaction between hydrogen and deuterium is the different position of the vibrational and rotational energy levels. The consequence of this difference is the existence of the isotope effect in the processes involving molecules, such as the dissociative electron attachment (DEA).

The simplest negative hydrogen production reaction, the radiative electron attachment to an atom:

$$H + e^- \rightarrow H^- + h\nu \tag{1}$$

played an important role in the origin of structures in the early Universe [34]. (The energy of the photon released in reaction (1) is equal to the electron binding energy (or electron affinity, EA) in the H^- ion). The formed H^- ions are then lost in an atomic hydrogen rich environment by associative detachment [34] to form hydrogen molecules:

$$H^- + H \rightarrow H_2 + e. \tag{2}$$

The theoretical study on the isotopic counterpart of reaction (2):

$$D^- + D \rightarrow D_2 + e \tag{3}$$

has been made by Chen and Peacher [35] and continued by comparing with experiments by Miller *et al* [36]. The cross sections for this process were first believed to show a difference between the two isotopes, but later it was clarifed that these crosss sections did not exhibit a large difference. Reactions (2) and (3) are the time reversed process of the DEA:

$$e + H_2 \rightarrow H^- + H \tag{4}$$

and

$$e + D_2 \rightarrow D^- + D \tag{5}$$

which are the fundamental processes producing H^- and D^- in ion source plasmas, as will be explained in detail in the next subsection.

The value determined using threshold-photodetachment spectroscopy by Lykke *et al* [37] for the EA of hydrogen is $6082.99\,cm^{-1}$ and that for deuterium is $6086.2\,cm^{-1}$ (i.e. 0.7542 eV for hydrogen and 0.7546 for deuterium). The low electron affinity is an advantage in that the H^- and D^- ions are easily neutralized after acceleration, but a disadvantage as they are also easily neutralized by collisions in the accelerator.

The D^- ions can be destroyed in the plasma volume by two-body recombination or mutual neutralization:

$$D^- + D^+(\text{or } D_2^+,\ D_3^+) \rightarrow \text{neutrals} \tag{6}$$

by photodetachment [38]

$$D^- + h\nu \rightarrow D + e \tag{7}$$

by collision with an electron

$$D^- + e \rightarrow D + 2\,e \tag{8}$$

or by collision with an atom

$$D^- + D \rightarrow 2\,D + e \tag{9}$$

and together with associative detachment (3) with specifying the vibrational level v''

$$D^- + D \rightarrow D_2(v'') + e. \tag{10}$$

Reaction (10) is also named associative detachment [36]. The inverse process (5) should be also dependent upon the initial vibrational level as well as rotational level, J, of the initial molecular state.

Negative deuterium ions are also formed in the plasma volume in a form of dissociative recombination of D_2^+ [39] and D_3^+ [40, 41] ions which leads to the production of an ion pair:

$$D_2^+ + e \rightarrow D^- + D^+ \tag{11}$$

$$D_3^+ + e \rightarrow D^- + D_2^+. \tag{12}$$

Other formation reactions requiring higher electron energy are polar dissociation [42, 43]:

$$D_2(v, J) + e \rightarrow D^- + D^+ + e \tag{13}$$

and dissociative attachment with formation of an excited atom

$$D_2(v,\ J) + e \rightarrow D^- + D^*. \tag{14}$$

D^- ions can also be produced in ion-molecule collisions such as:

$$D_2^+ + D_2 \rightarrow D^- + D + 2D^+ \tag{15}$$

$$D_2^+ + D_2 \rightarrow D^- + D^+ + D_2^+ \tag{16}$$

when molecular ions with high enough energies are present.

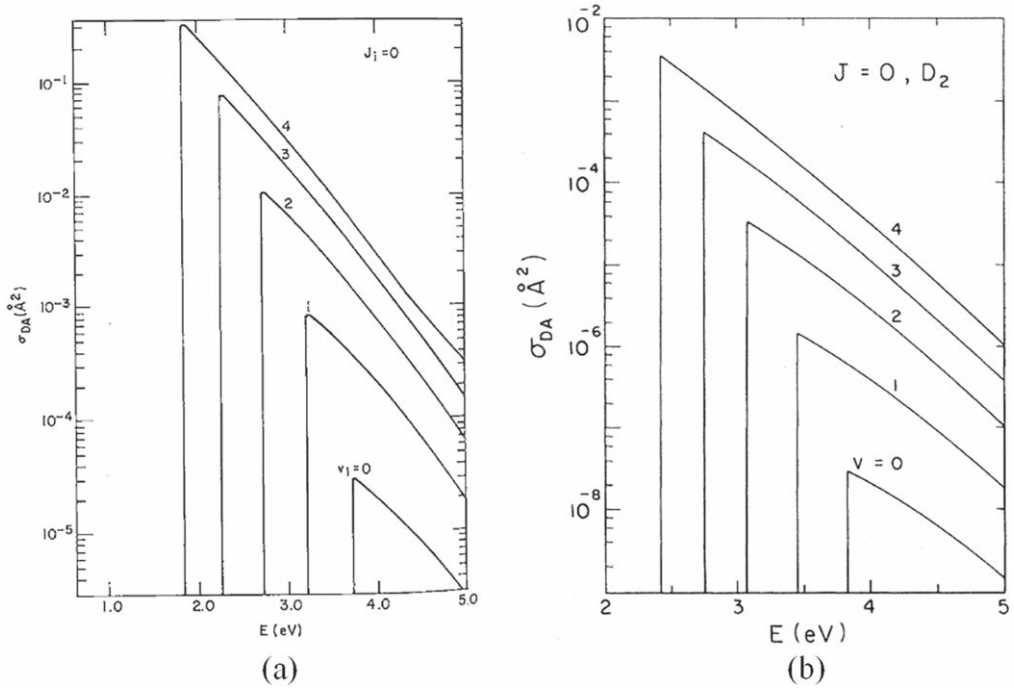

Figure 1. Illustration of differences in threshold and peak values of dissociative electron attachment cross sections between (a) hydrogen and (b) deuterium. Figure 1(a): figure 1 of [51], J M Wadhera, J N Bardsley 1978 *Phys. Rev. Lett.* **41** 1795, and figure 1 (b): figure 3 of [52], J N Bardsley and J M Wadhera 1979 *Phys. Rev.* A **20** 1398. Reused with permission from the American Physical Society.

Reaction probabilities and their dependence on the vibrational and rotational quantum numbers

The production of H^- ions in the DEA process $e + H_2 \rightarrow H + H^-$ was first observed 60 years ago by Hvostenko and Dukelskij [42, 43] and studied later in detail by Schulz and Asundi [44]. The existence of an isotope effect in negative hydrogen ion formation by dissociative electron attachment has been predicted theoretically by Demkov [45] and by Chen and Peacher [35] while it was demonstrated experimentally by Schulz and Asundi [46] and Rapp *et al* [47]. Allan and Wong [48] and later Orient and Chutjian [49] showed experimentally that the DEA cross sections varied with the rovibrational states of the molecule and were also isotope dependent thus confirming the theoretical predictions of Wadhera and Bardsley [50, 51] and Gauyacq [52].

In the deuterium plasma volume the negative deuterium ions (D^-) are formed mainly by DEA of a low-energy (cold) electron to an excited molecule at vibrational level v' and rotational level J:

$$D_2(v',\ J) + e \rightarrow D + D^-. \qquad (17)$$

We denote here (low energy electrons) the electrons with the energy below 4 eV. The reason why low energy electrons are required for the formation of negative deuterium ions by DEA, reaction (17), can be understood from figure 1, where the electron energy dependence of the DEA cross sections for H_2 and D_2 calculated by Bardsley and Wadhera [51] is shown. These calculations have been done vibrationally resolved only. This DEA cross section is maximum at the threshold energy. The threshold energy is highest for $v' = 0$ and goes down with increasing v'.

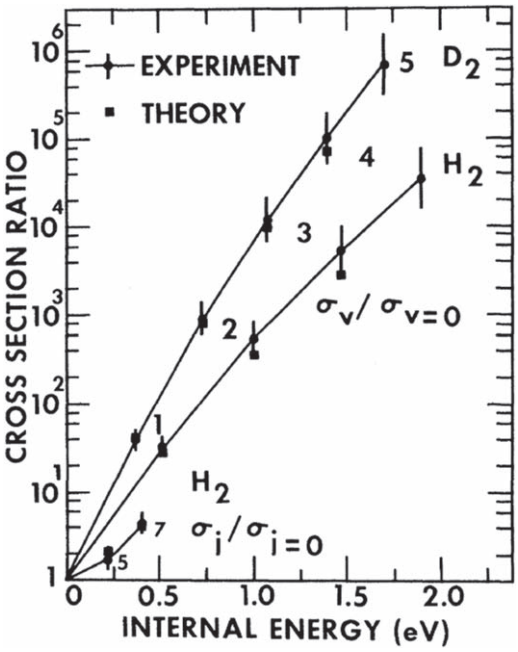

Figure 2. Internal-state dependence of threshold dissociative attachment cross sections in H_2 and D_2. (Figure 3 of [49] M Allan, S F Wong 1978 *Phys. Rev. Lett.* **41** 1791.) Reused with permission from the American Physical Society.

The data shown on figure 1, clearly indicate the difference in threshold energy and peak cross sections between H_2 and D_2. The comparison of these theoretical results with the experimental data of Allan and Wong [48], is shown on figure 2. On this figure the peak DEA cross sections are plotted as a function of the internal energy of each

vibrationally and rotationally excited state. These cross sections were derived for individual vibrational and rotational states from experimental spectra (i.e. H^- and D^- ion current versus electron energy) measured using an electron-impact mass spectrometer. Vibrationally and rotationally excited molecules were generated in a hot iridium collision chamber. The experiment consisted of measuring the energy dependence in the 1 –5 eV region for the dissociative attachment in H_2 and D_2 at temperatures ranging from 300 to 1600 K. It was assumed that the populations of vibrational and rotational states are given by Maxwell–Boltzmann distribution.

Wadhera [53] reported the rates of DEA to rovibrationally excited H_2 and D_2. He showed that the attachment rate depends almost on the total internal energy and not on the specific partition of internal energy between vibrational and rotational modes. As the internal energy is increased beyond 3.994 eV for H_2, the dissociative attachment process becomes exoergic and the attachment rate becomes about $10^{-8}\,\mathrm{cm^{-3}\,s^{-1}}$, almost independent of the electron temperature.

Calculated results of cross-sections using the resonant model for electron-impact inelastic processes, including DEA to vibrationally excited molecules of hydrogen and its isotopes deuterium and tritium were reported by Celiberto *et al* in *Atomic Data and Nuclear Data Tables* [54]. Capitelli *et al* [55] reported cross sections of elementary processes relevant to negative ion kinetics, including electron-molecule and atom-molecule interactions, emphasizing the role of vibrational excitation in affecting the cross sections. Fabrikant *et al* dedicated a review to the theoretical study of DEA in molecular hydrogen [56]. Horacek *et al* [57] reported calculation results of DEA based on an improved nonlocal resonance model. A detailed discussion of the DEA cross section as a function of the target vibrational and rotational states is given by Horacek *et al* [57] and they show that for high values of the rotational excitation level of the hydrogen molecule the DEA cross sections are larger than those for high vibrational excitation levels. According to these authors the largest dissociative attachment cross section of $28.3 \times 10^{-16}\,\mathrm{cm^2}$ is obtained for $v' = 1$ and $J = 29$. Horacek *et al* also investigated the isotope effect, and showed that the enhancement in cross section at high rotational levels was smaller for D_2 compared to that at high rotational levels in H_2 [57]. It is important to note that the DEA cross sections for D_2 are smaller than those for H_2. It is not clear to what extent these results are affected by not taking into account the nuclear spin. Therefore, further research should be dedicated to this subject.

Note that the cross sections for deuterium molecule dissociation (equation (18)) and ionization (equations (19) and (20)) are also different from these cross sections for hydrogen.

$$\mathrm{D_2}(v,\ J) + \mathrm{e} \rightarrow 2\,\mathrm{D} + \mathrm{e} \tag{18}$$

$$\mathrm{D_2}(v,\ J) + \mathrm{e} \rightarrow \mathrm{D} + \mathrm{D^+} + 2\mathrm{e} \tag{19}$$

$$\mathrm{D_2}(v, J) + \mathrm{e} \rightarrow \mathrm{D_2^+} + \mathrm{e}. \tag{20}$$

The difference in the volume production rate of deuterium negative ions $(\mathrm{d}n_{D^-}/\mathrm{d}t)_{vol\ prod}$ in the deuterium plasma compared to the volume production rate of hydrogen negative ions in the hydrogen plasma, is due to two factors: (a) the cross sections of DEA, σ_{DA}, to the different rovibrationally excited states of the D_2 molecules [48, 49] are lower than these cross sections for the H_2 molecules; (b) the higher plasma potential of the deuterium plasma due to its higher electron temperature and its heavier positive ions [58, 59]

The investigation of the difference in the negative ion production between hydrogen and deuterium, i.e. the isotope effect, in the production of hydrogen negative ions is important from the view point of fundamental plasma physics as well as from the view point of atomic and molecular physics. Due to the larger mass of the deuterium atoms (D°) their velocity, v, is smaller than that of hydrogen atoms (H°) of the same energy by a factor $\frac{1}{\sqrt{2}}$:

$$v(\mathrm{D}^\circ) = \frac{1}{\sqrt{2}} v(\mathrm{H}^\circ). \tag{21}$$

Ions in deuterium plasma traverse magnetic fields with their Lamor radii larger than hydrogen ions and thus may shorten the confinement times of plasma confinement devices. This is one reason why the intensity of the magnetic filter field separating the extraction region plasma from the driver region plasma may require an adjustment for switching the gas from hydrogen to deuterium.

Negative ion production processes at a surface in plasma

Ions can pick up electrons at the surface to be neutralized, while atoms with the positive value of electron affinity can trap an extra electron to the affinity level at the surface collision to become negative ions. Due to their small values of electron affinities, 0.7542 eV for hydrogen and 0.7546 for deuterium, H^- and D^- ions can lose their electron to a level of the surface conduction band and the negative ion becomes neutralized. The affinity level is lower than the conduction band edge in the classical model of image potential, when the distance x between the surface and the negative ion is smaller than the following value:

$$x = \frac{e^2}{8\pi\varepsilon_0(\phi_w - E_A)}, \tag{22}$$

where e is the unit charge, ε_0 is the permittivity of vacuum, E_A is the electron affinity and ϕ_w is the work function. When the surface work function is high, the affinity level exceeds the band edge at a smaller distance and the probability for the negative ion to lose the electron becomes large. For a low work function surface, the negative ion can reach larger distance and it remains as a negative ion. This formation process of negative ions by electron capture at low work function surface, is often called surface production or negative ionization [60].

Low work function materials are indispensable for surface production and alkali metals, particularly Cs adsorbed on refractory metals are known to exhibit low work functions. This is because caesium has the lowest ionization potential to

make the largest electric dipole moment when it is adsorbed on metal surface. As Cs atoms are deposited on a surface of Mo, the material commonly used for extraction grids for ion source, the work function decreases from about 4.6 eV for pure Mo. Ernst-Vidalis *et al* measured the work function change of pure Mo in his ultra-high-vacuum (UHV) system and reported that the work function took the minimum at about 1.5 eV with 0.17 monolayer Cs coverage and reached a saturation value about 2.1 eV for bulk Cs above 0.36 monolayer coverage [61]. Thus, Cs coverage on the metal suface should be controlled to keep the work function to be minimum.

Another important factor that determines negative ion fraction β^- of particles leaving the surface is the normal velocity component v_z. When a negative ion passes through the region near the surface the affinity level electron can make the transition to a level of the surface conduction band and the negative ion becomes neutralized. Rasser *et al* [60] showed that their equation derived from a quantum mechanical model can be reduced to the following simple formula to compute β^-, which was derived by Blandin *et al* for small v_z cases [62]:

$$\beta^- = \frac{2}{\pi} e^{-\frac{\pi(\phi_W - E_A)}{2av_z}}. \tag{23}$$

Here a is the exponential decay constant of the transition rate at large distance. One should note that this equation shows the existence of an isotope effect; the β^- for deuterium should be lower than that for hydrogen provided the isotopes escape the surface with the same energy.

The quantum mechanical model calculation to estimate β^- was first reported by Kishinevskii [63]. Rasser *et al* described the negative ionization from clean tungsten, caesiated tungsten and thick caesium surfaces at low energies with two models: a probability model and an amplitude model [60]. In both models the electron motion is described quantum mechanically and the nuclear motion classically. The electron affinity level of an atom close to the metal is lowered by image forces and broadened due to the resonant transition of an electron between the conduction band of the metal and the valence shell of the atom. Rasser's results predict lower β^- than Kishinevskii's model, as they have included the effect due to density of states near the surface. The maximum negative ionization efficiencies calculated by Rasser *et al* are 4% on W(110), 40% on caesiated tungsten and 15% on caesium.

Hiskes *et al* discussed the kinetic energy necessary for negative ions to leave the surface: 0.77 eV for Cs, and 1.25 eV for sodium [64]. This energy should be provided through a particle reflection process, or a sputtering process of adsorbed atoms. The particle reflection coefficients R_N and the energy reflection coefficients R_E are dependent upon the mass of the incident ions or neutrals as tabulated by Eckstein [65]. The sputtering yields of adsobed hydrogen isotopes together with the velocity distribution of the desorbed isotope atoms are different between hydrogen and deuterium.

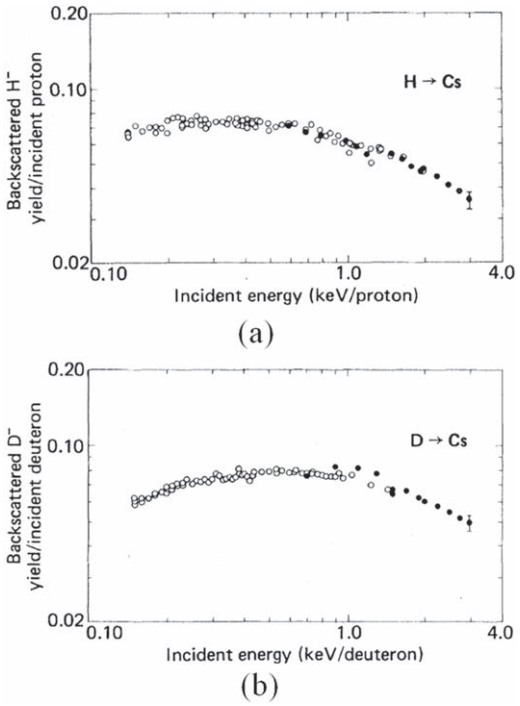

Figure 3. Back scattering negative ion yields of (a) H^- and (b) D^- from thick Cs adlayer. (Figures 4 and 5 of [68]: P J Schneider *et al* 1981 *Phys. Rev.* B **23** 941.) Reused with permission from the American Physical Society.

Production rate for backscattered and sputtered hydrogen isotope negative ions

The dependence of negative ionization efficiency upon incident H/D energy was experimentally confirmed for the reflection process at alkali metal surfaces by Hiskes and Schneider [66]. They prepared clean alkali metal surfaces by depositing thick layer (more than several monolayers) of alkali metals on a cooled metal target contained in an UHV system. The surface was bombarded by hydrogen and deuterium atomic/molecular beams and the amount of produced negative ion current was measured to obtain the negative ion yield. They have observed clear shifts of the maximum negative ion yields to higher incident energies by switching the isotope ions from hydrogen to deuterium: energy dependence of β^- corresponding to difference in isotope mass. This dependence is clearly observed in figure 3, which was reported by Schneider *et al* using the same experimental device [67]. They showed that the peak D^- fraction in the beam of D_2^+ ions backscattered from clean Cs surface was comparable to the peak H^- fraction in the beam of H_2^+, but the D_2^+ ion incident energy that realized the peak fraction was higher than the H_2^+ ion incident energy corresponding to the peak H^- fraction.

Negative ions of H and D can be surface produced through reflection of thermal/Frank-Condon neutrals. Ion induced desorption of surface adsorbed H/D provides small kinetic energies to the produced negative ions, which should show the effect of outgoing velocity dependence upon the isotope mass difference. Yu bombarded his Mo (100) sample contained in his UHV system with Ne^+ ions from 150 eV to

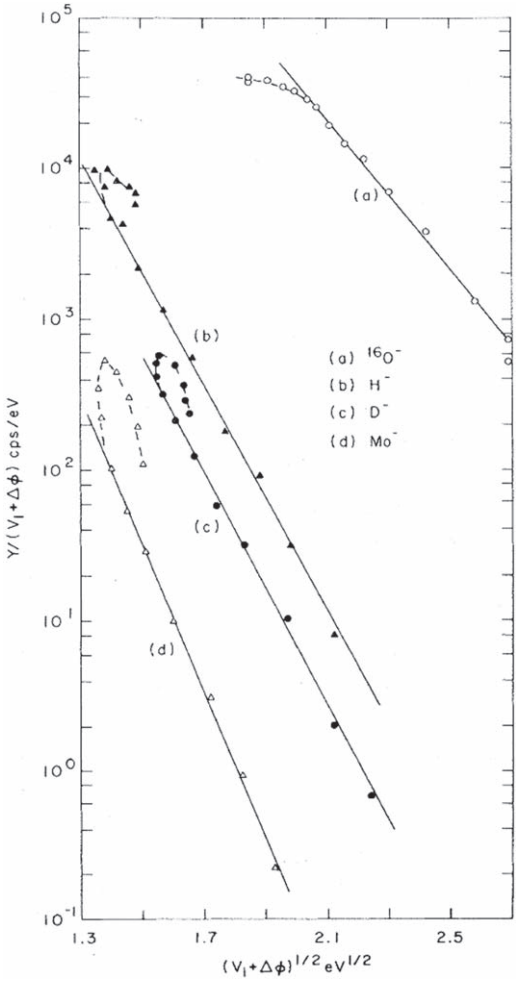

Figure 4. Illustration of the difference in negative ionization efficiency after Yu. (Figure 2 of [70]: M L Yu 1978 *Phys. Rev. Lett.* **40** 574.) Reused with permission from the American Physical Society.

3.5 keV energy to measure H and D negative ion yields [69]; surface adsorbed H and D were sputtered by Ne^+ ions and part of them were negatively ionized. A H/D overlayer was formed on the pure Mo sample by introducing the gases into the vacuum system, and the Cs was deposited on the hydrogen isotope adsorbed sample. Yu found the efficiency to produce D^- ions was about one order of magnitude lower than the efficiency to produce H^- ions for the same work function condition, as shown in figure 4. This isotope effect can be attributed to the smaller D^- ion normal velocity component with respect to the low work function surface than the H^- ion normal velocity component. Another way to investigate the negative ionization efficiency at smaller velocity is to use thermal atoms of hydrogen isotopes. Surface production of D^- ions by directing H/D atoms produced by a tungsten furnace to a low work function surface was attempted by Graham [68]. Keeping the tungsten tube furnace temperature at 2500 K, he found that the rapid increase in negative ion signal counts was correlated to the reduction of work function of the Cs covered polycrystalline Mo surface. However, the yield was too small to make a quantitative comparison in the efficiency between hydrogen and

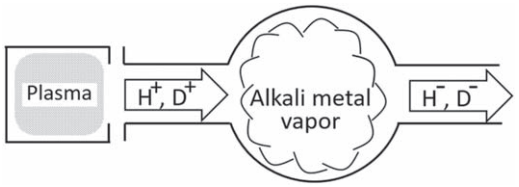

Figure 5. A schematic showing a double charge exchange type negative ion source.

deuterium atoms [68]. Surface negative ionization efficiency for thermal deuterons is expected to be lower than 1.5×10^{-4} ions per incident atom, which was measured for hydrogen atoms by Pargellis and Seidl with their tungsten oven temperature maintained from 1800 to 2400 K [70].

Historical review of H^-/D^- sources

Some reaction cross sections of deuterium molecules are different from those of hydrogen molecules. Thus, the negative ion densities in plasmas can be different between hydrogen and deuterium. On the other hand, beams of H^- and D^- can be also produced through processes other than collisions in plasmas. The history of beam sources of D^- started from double charge exchange sources, continued with surface conversion and volume sources. This section describes how the D^- source development has been advanced.

Double charge exchange sources

The original concept of D^- ion source was to form an H^-/D^- ion beam starting from proton/deuteron beams. High density neutrals in the volume of charge exchange cell transfer electrons to the positive ion beam and the produced neutral beam to convert them to a negative ion beam. The charge exchange cell forms the heart of the structure of a double charge exchange type negative ion beam source (see figure 5 for a schematic presentation). Enough target thickness, or the line integrated density, has to be achieved to obtain a negative ion beam of sufficient intensity. Meanwhile, the target thickness should be kept below some thickness as a part of the produced negative ions will be lost due to scattering collisions.

Donnally *et al* [71] pointed out that the maximum cross section for charge-exchange is large when the energy defect and the ionization energy of the atoms are small (the energy defect is the change in the total internal energy of the system as a result of the charge-exchange collision). Therefore, a better choice of the atom from which the proton could gain an electron is ceasium, since in the case of the charge-exchange with caesium the energy defect is only 0.43–0.49 eV and the ionization energy of caesium is only 3.89 eV in contrast to an energy defect of 12 eV and an ionization energy of 15.44 eV for H_2.

The charge exchange of 10–30 keV protons on thick vapor jets of lithium, sodium, magnesium and zinc was studied by Dyachkov and Zinenko [72] in a small accelerator in which the charge exchange target was contained in a cube

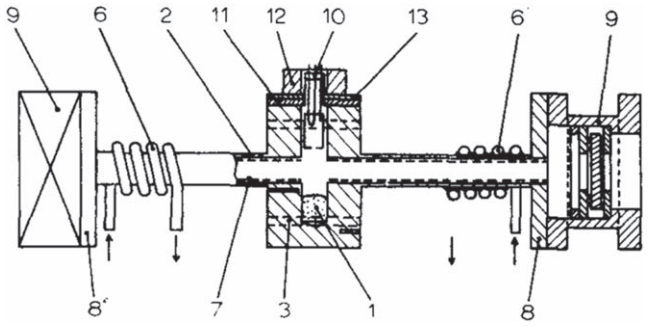

Figure 6. Vertical section of the cesium charge-exchange cell. 1: cesium reservoir; 2: charge-exchange canal; 3: heater; 6: copper coils brazed to the extremities of the cell; 7: wick; 8: flange; 9: slide-valve; 10: surface ionization gauge; 11: flange supporting the surface ionization gauge; 12: oven; 13: asbestos sheet. (Figure 1 of [75].) With permission from M Bacal *et al* 1974 *Nucl. Instrum. Methods* **114** 407, ELSEVIER.

($35 \times 35 \times 35$ cm^3). Dyachkov *et al* [73] measured the maximum conversion yield in the energy range from 1 to 10 keV and reported that this yield increased, as was expected, with the decreasing ionization potential of the target atom. The measured results are 4.2% for Mg, 5.3% for Li and 9.5% for Na. For K, the maximum conversion yield is located below 1 keV and it is clear from the curve that the maximum value of the conversion yield for K is larger than that for Na.

Bacal and Reichelt [74] proposed a new method for confining a metal vapor at a pressure of about 10^{-3} Torr, with extremely low loss of metal into the vacuum chamber surrounding the metal target. This method consists in recycling the liquid metal: condensation of vapor in the charge exchange target to the liquid state, its return to the high pressure region being ensured by capillarity. Due to the similarity of its operation to that of a heat-pipe, this charge-exchange cell is sometime denoted as 'recirculating metal-vapor (heat-pipe) target'. This idea was demonstrated by the experiment of Bacal *et al* [75] using Cs in the cell configuration shown in figure 6. The charge-exchange canal (2) is a tube of stainless steel, 1.8 cm in diam and 30 cm long. The walls of the central region of this tube are very thick (outer diameter 10 cm), so that they house the metal reservoir and a heater. The return of the liquid metal to the reservoir by capillarity was made possible by ensuring that (1) the temperature of the colder part of the canal should be higher than the Cs melting point (28.5 °C) and (2) caesium condensing on the inside diameter of the charge-exchange canal will be spread out by the wick (7 in figure 6). The wick is formed of 3–4 layers of stainless-steel wire cloth spot-welded together and set in the canal in close contact with the wall. This design was adopted in several commercial Tandem accelerators, but also in experimental studies of D^- production by charge transfer (e.g. Schlachter *et al* [76]) and for generation of intense sodium atomic beams for use in laser cooling experiments (e.g. Vestergaard Hau *et al* [77]).

A large size deuterium negative ion charge exchange source was studied by Delaunay *et al* [78] in view of a deuterium neutral beam for the Grenoble project proposed by Geller *et al* [79]. A supersonic jet of Caesium was built for this project [80]: a high density flow of alkali-vapor was produced for a large diameter, high curent beam source. A recycling system collected the alkali metal liquid from condensers to put it back into the oven where the caesium vapor is produced (figure 7).

Grübler *et al* [82] reported the equilibrium charge components, F_-^∞, in Cs, K, Na and Li vapor as a function of incident proton and deuteron energy. Their results reveal that the beam energies at which F_-^∞ take maxima shift from Cs to Li. The value of the maxima decreases from Cs to Li monotonically from approximately 0.21 at 0.75 keV to 0.06 at approximately 3 keV. Their comment is that 'it seems at first that Cs should be the most powerful charge exchanger'. However, the production of a 0.75 keV high intensity hydrogen beam and the transport to the charge exchanger is a difficult task. The choice of sodium as a charge exchanger has the great advantage that the incident beam can have a much higher energy without too great a loss in the charge exchange yield.

Schlachter *et al* reported results on the D^- production by multiple charge-transfer collisions and the D^- equilibrium fraction in Cs, Rb, Na, Mg and Sr vapor in the energy range 0.3–20 keV (see figure 8) [76]. These results were obtained in a device in which the ion beams of interest, i.e. deuterium positive or negative ions, were directly extracted from one or two duoplasmatron ion sources and directed through a recirculating metal-vapor (heat-pipe) target as shown on figure 6. They showed that the equilibrium D^- fraction in caesium vapor reached the maximum value of 35% at energies below 500 eV, as shown in figure 8. This is also true in rubidium vapor, with an equilibrium D^- charge state fraction somewhat lower than 30%, but not in Na, Mg and Sr. These results support the mentioned strategy proposed by Grübler *et al* [82] i.e. preferring the use of another metal rather than the use of caesium. Therefore, a lithium vapor target is used in tandem accelerators for the double charge exchange of the accelerated D^+ ion beam to a D^- ion beam. Note that in the tandem accelerator the deuterium beam is accelerated by the same applied voltage to double the energy, first as a positive ion beam, then after the double charge exchange, as a negative ion beam. In Li vapor the equilibrium D^- fraction reaches reasonably high values at higher D^+ energy.

The work of Osher *et al* [81] was the first demonstration of an intense beam produced by charge exchange in a Cs target: 50 mA of D^- ions. At the 1977 Symposium in Brookhaven the fusion oriented laboratories from the US, Russia and France reported their efforts in building large negative ion sources and test facilities based on the double charge exchange process. Hooper *et al* [83] reported the acceleration to 60 keV of a D^- ion beam with current larger than 100 mA, produced by double charge exchange in a Cs target. Semashko *et al* [84] reported the achievement of a negative ion current of 1.4 A at an energy of 40 keV by double charge exchange in a sodium (Na) target. Poulsen and Hooper demonstrated the production of 2 A of D^- ion current extracting 26 A positive ion current at 10 kV [85] using the Berkeley 50 A positive ion source developed by Ehlers and Leung [86] coupled to the cell of supersonic sodium vapor jet

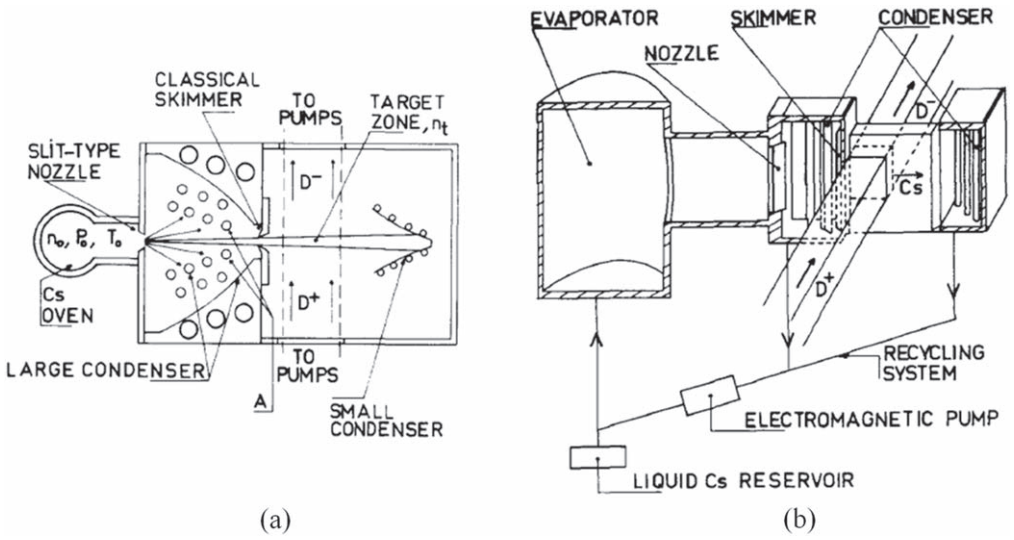

Figure 7. Schematic diagram showing (a) super-sonic-jet-type alkali metal target cell, and (b) components for Cs recycling. (Figures 4 and 5 of [81].) Reproduced from the article by M Bacal *et al* 1982 *Rev. Sci. Instrum.* **53** 159 with the permission of AIP Publishing).

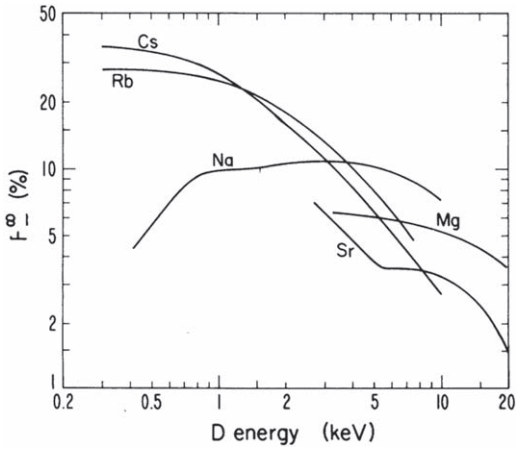

Figure 8. Equilibrium charge state fraction for different metal vapor targets versus incident D^+ ion energy. (Figure 13 from [78]: A S Schlachter *et al* 1980 *Phys. Rev.* A **22** 2494.) Reused with permission from the American Physical Society.

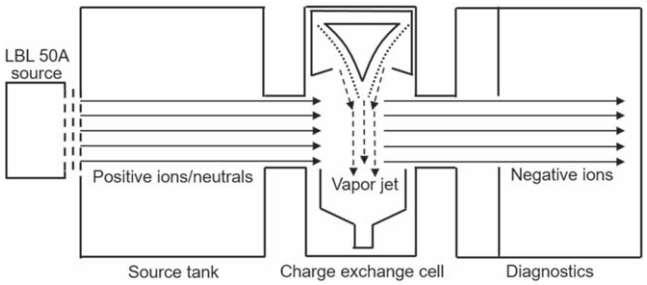

Figure 9. Schematic illustration of the large size double charge exchange negative ion source demonstrated by Hooper *et al* [85]. Reproduced from the article 'High current D^- production by charge exchange in sodium' by E B Hooper *et al* published in *J. Appl. Phys.* **52** 7027 (1981) with permission of AIP Publishing.

as shown in figure 9. This system converted positive ions extracted from the source with the 7 cm × 35 cm extraction grid area to focus the beam at a distance of 3 m.

Geller *et al* [79, 87] announced their plan to associate a microwave positive ion source with a caesium vapor charge exchange cell described by Bacal *et al* [80] to produce 0.4 A of D^- ions with a current density of 15 mA cm^{-2}. Morgan [88] studied the D^- ion formation by double-electron capture in alkaline-earth vapor targets, namely the double electron capture producing D^- ions in magnesium and barium vapor targets.

Three years later, at the Second International Symposium in Brookhaven, Hooper *et al* reported that 2.2 A of D^- ion curent were produced with a Sodium target at 12 keV [89, 90]. They also investigated the design of a Rb cell to achieve a total current of 20 A with 23 mA cm^{-2} current density with the extremely low D^- energy of 1.5 keV [90].

Delaunay *et al* [78] described the production of D^- ions by double charge exchange of D^+ ions on a supersonic jet of Cs (shown on figure 7) developed by Bacal *et al* [80]. The choice of the supersonic jet of Cs was made for meeting the need to minimize the mean free path of the D atoms involved. Vapor targets of Na and Cs were the proper options depending upon the design of the low energy beam transport sections as can be seen in the graph of equilibrium negative ion charge state fraction, F_-^{∞}, shown in figure 8. Cs shows the maximum at low energy, while Na shows the maximum at high energy.

The optimization of the H^- system directly leads to the D^- system in the double charge exchage system except the positive ion source performance; the extractable current together with the atomic/molecular ion species govern the overall positive ion beam output, and the high performance positive ion source is the key in the double charge exchange negative ion source system. The main problem associated with the double charge exchange negative ion beam system is the complexity to realize the post accelerator by forming a high energy beam from the negative ions produced by the

double charge exchange system installed on the high voltage terminal.

Volume sources

While the first approach to produce the required D^- beams was made through charge transfer processes in metal vapor, the demonstration of the existence of volume production of H^- and D^- ions [91] changed the direction of research and development to physical processes that would lead to the generation of D^- ions in low-pressure D_2 plasma. At the first international symposium in Brookhaven in 1977, Bacal *et al* at Ecole Polytechnique reported the observation of an anomalously large concentration of negative ions present in a hydrogen discharge at low pressure (in the range 10^{-4}–10^{-3} Torr) [92, 93]. and proposed an interpretation of this finding. This anomaly has been studied both experimentally and theoretically at several laboratories, in particular at LBL [94, 95] (Lawrence Berkeley Laboratory) and the efficient production of H^- ions in the volume of a plasma produced at low pressure was confirmed. The analysis of these discharges led to a working hypothesis for a formation process in which the hydrogen molecules are first vibrationally excited in collisions with energetic electrons, and subsequently capture thermal electrons which leads to dissociative electron attachment. This formation process was soon designated as volume production and the corresponding source, as volume source. At the fifth international symposium in Brookhaven in 1990 Elizarov *et al* [96] described a negative ion volume source with caesium additive. These two types of volume sources will be described in this section.

Volume source operation without Cs

The measurement of the negative ion density by photodetachment [38] in H_2 and D_2 gas in a multi-cusp (bucket) source with the electron density in the range 10^9–$10^{10}\,\mathrm{cm}^{-3}$ showed no isotope effect [91], but confirmed the presence of a significant density of negative ions in a plasma produced at low pressure, as reported first by Nicolopoulou *et al* [92, 93]. Since the invention of the magnetic filter by Ehlers and Leung in 1981 for controlling positive ion species in the LBL positive ion source [94, 95] the negative ion source is often divided by a magnetic filter into a source chamber (or driver) and an extraction chamber. It was shown by Leung *et al* [97, 98] that the ion source structure shown in figure 10 with the magnetic filter and a small positive bias to the plasma electrode (single aperture plasma grid) can produce a very significant reduction in the electron current and a significant increase of the extracted volume-produced H^- ions. McAdams and Holmes have introduced the magnetic filter into the Culham Laboratory negative ion source [99]. These authors indicate that its role is to separate the driver containing the energetic electrons (necessary for ionizing the gas, equation (20) and producing the vibrationally and rotationally excited molecules), from the extraction chamber characterized by a low electron temperature favorable for the production of H^-/D^- by DEA (equations (4) and (5)). The extraction

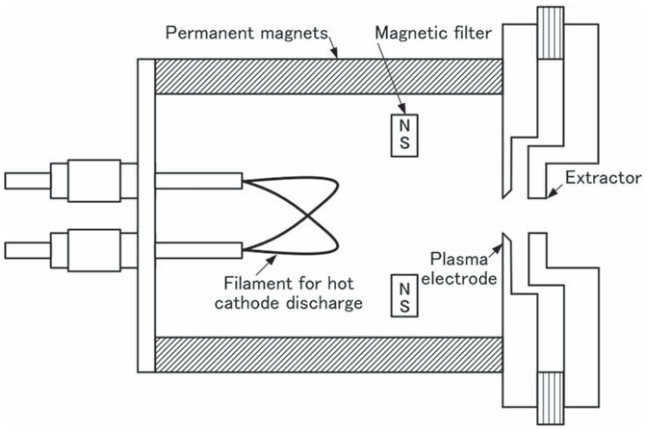

Figure 10. A schematic illustration of a multicusp plasma source with magnetic filter based on figure 1 of the article by K N Leung and K W Ehlers 1984 *AIP Conf. Proc.* **111** 67, figure 1, [99], with the permission of AIP Publishing.

chamber plasma density is typically 50 times lower than the driver plasma density, while its electron temperature is 3–5 times lower.

The structure of a typical H^-/D^- ion source with a magnetic filter is schematically shown in figure 10. Due to the lower electron density and temperature in the extraction chamber compared to that in the driver the amount of electrons extracted and accelerated is reduced while an efficient negative ion production by the DEA process takes place. By the addition of the magnetic filter field, another factor causes a difference in source performance between hydrogen and deuterium operation: due to the larger Larmor radius for the same kinetic energy, deuterium ions can traverse the magnetic filter field more easily than hydrogen ions. The Larmor radius R_L of an ion of mass M is calculated by the following equation:

$$R_\mathrm{L} = \frac{Mv_s}{eB} = \frac{\sqrt{MkT_e}}{eB}, \tag{24}$$

where k is the Boltzmann constant, T_e is the electron temperature. The transport of ions from the driver to the extraction chamber is enhanced by the increase of ion Larmor radius proportional to the ratio $\sqrt{M}/B$ with B being the intensity of the magnetic field. Electrons with their much smaller Larmor radius do not directly reach the extraction region from the driver region, but electrons are replenished in the extraction region to keep the quasi neutrality of plasma. This enhanced plasma transport for larger Larmor radius condition was confirmed by the experiment varying the intensity of the filter magnet [98]. The intensity of the filter field must be adjusted for enhancing DEA while reducing H^- destruction by electron collisions. Thus, it is necessary to use a $\sqrt{2}$ times stronger magnetic field in the deuterium plasma with the same electron temperature as the hydrogen plasma in order to maintain the same Larmor radius as in the hydrogen plasma and obtain a proper magnetic filtering.

The changes in the plasma parameters associated with H_2 working gas replaced to D_2 were studied using different size multicusp plasma sources, 25.4 cm diameter 23.6 cm depth

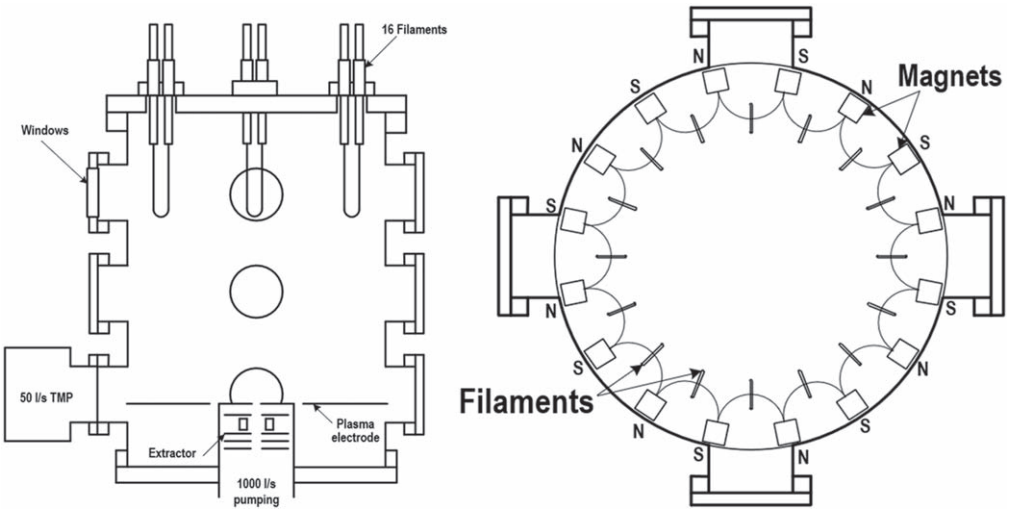

Figure 11. Schematic presentation of the plasma volume source CAMEMBERT III (Figure 1 from [60], A M Bruneteau *et al* 1996 *Rev. Sci. Instrum.* **67** 3827.) Reproduced with the permission of AIP Publishing.

Camembert II and 44 cm diameter 45 cm depth Camembert III developed at Ecole Polytechnique (Palaiseau, France) described by Bruneteau *et al* [58]. Figure 11 shows the schematic illustrating Camembert III ion source equipped with 16 arc discharge filaments negatively biased by 50 eV with respect to the metal walls. The thermionic electrons emitted by these filaments, after acceleration to 50 eV, ionize the gas and produce the rotationally–vibrationally excited H_2 and D_2 molecules. The choice of the position of these filaments in the multicusp magnetic field avoids the need of a magnetic filter, since the energetic electrons are confined close to the walls. The central region of the plasma represents the extraction region. The operation of this plasma source is explained by Courteille *et al* [59] and in the review by Bacal *et al* [100].

The difference in the negative ion density in hydrogen and deuterium is illustrated in figure 12, where it is shown that at low discharge current there is no difference in negative ion density between H_2 and D_2 but this difference, i.e. the isotope effect, develops with the increase of the discharge current [58]. This is explained by the increase with the discharge current of the density of atomic hydrogen, which was reported by Livshits *et al* [101].

Leroy [17, 18] and Skinner *et al* [19] showed that the difference in plasma density between the source operated in H_2 and D_2 was negligible, but there were differences in electron temperature, T_e: for a gas pressure of 3 mTorr the ratio of the electron temperatures $T_e(D_2)/T_e(H_2)$ is independent of the discharge voltage and has a value of 1.2. Running the discharge in D_2 and H_2 at the same pressure of 3 mTorr they found that in the larger source Camembert III the maximum D^- density measured at the discharge current of 80 A was approximately 53% of the maximum H^- density [17, 18]. The difference between the densities of H^- and D^- is larger in Camembert III compared to Camembert II, i.e. it increases with the source size. Péalat *et al* showed that this was related to the larger density of atoms in the larger source and to the higher discharge current [102]. Leroy has also shown that

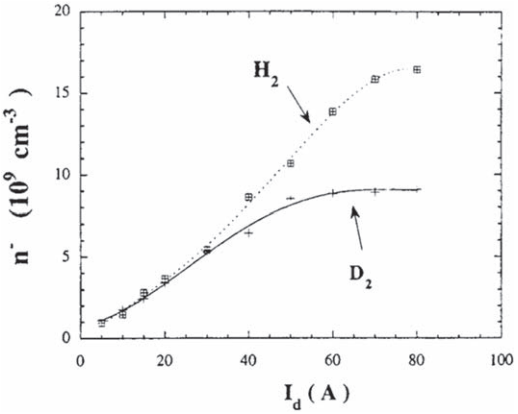

Figure 12. Comparison of the dependence of the negative ion density versus the discharge current in the large volume source Camembert III at a gas pressure of 3 mTorr, with a discharge voltage of 50 V (Figure 8 in [60]: A M Bruneteau *et al* 1996 *Rev. Sci. Instrum.* **67** 3827.) Reproduced with the permission of AIP Publishing.

there was no large difference between the co-extracted electron currents in H_2 and D_2 in ion source operation at moderate power [17], like in Camembert III (less than 10 kW).

When the negative ion density in the smaller source, Camembert II, is plotted versus the electron temperature, both H^- and D^- densities attain a maximum in the electron temperature range 0.6–0.8 eV as shown in figure 13, while the maximum density is again smaller for D^- [18]. Not only the electron collision reaction rates, but also rate coefficients of collisions with other plasma species determine the final H^- and D^- ion densities.

Fukumasa *et al* compared the volume production of H^- and D^- ions in his 16 cm diameter 30 cm long double plasma type multicusp source and found that the optimum pressure was two times higher for deuterium (3 mTorr) compared to hydrogen (1.5 mTorr) [20]. The required magnetic filter field intensity to obtain the largest negative ion current was larger for the case of deuterium operation. This result is due to the

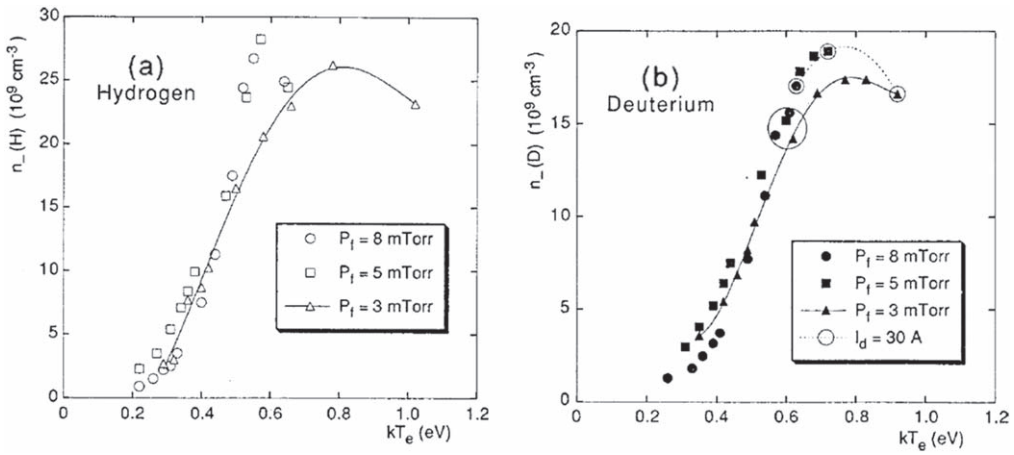

Figure 13. Negative ion densities obtained by changing pressure plotted as functions of measured values of electron temperature, kT_e, at the center of the plasma of the Camembert II ion source. (Figure 13, [20].) Reused with permission from the American Physical Society.

need of maintaining the same Larmor radius in the deuterium plasma as in the hydrogen plasma, in order to obtain a similar filtering effect (see equation (24)). This result was confirmed by Inoue *et al* [103] when they studied the JAERI magnetically filtered multi-cusp source, the 36 cm long, 21 cm wide 15 cm deep arc discharge 'one-ampere negative ion source' which was operated at LBL. The magnetic filter field strength can be varied from 450 to 910 G cm by changing the sizes and number of the filter permanent magnets. They have also found that the lowest electron to negative ion current densities ratio at the optimum magnetic filter strength was equal to 13 for hydrogen, and equal to 38 for deuterium [103], i.e. more electrons were extracted with D^- than with H^-. They also found that the positive plasma grid bias potential needed for decreasing the co-extracted electron current was higher for deuterium operation than that needed for hydrogen operation. They attributed this to the lower ion loss rate in deuterium plasma, due to the smaller ion velocity of deuterium compared with hydrogen because of the larger ion mass. They assumed that the same extraction conditions, or the same loss rate of positive deuterium ions and electrons, as in the case of hydrogen operation were obtained in deuterium operation by applying a larger positive bias to the plasma grid.

According to Svarnas *et al* [104] the value of the co-extracted electron current becomes negligible when the plasma grid potential is biased sufficiently positive (by 1–2 eV) against the plasma potential. This was confirmed by numerical modeling by Kuppel *et al* [105]. The potential difference between the plasma and the facing wall is approximately equal to the difference between the plasma potential, V_p, and the floating potential, V_f, which depends on the ratio of the positive ion and electron masses, M/m:

$$V_p - V_f = \frac{kT_e}{2} \ln \frac{2M}{\pi m}. \tag{25}$$

Therefore, $V_p - V_f$ depends on the gas isotope flowing into the plasma through two factors: the electron temperature and the mass of the positive ions. Assuming atomic positive ions in both hydrogen and deuterium plasmas, the ratio M/m will be two times larger in the deuterium plasma than in the hydrogen plasma, namely $M_d/m = 3672.304$ and $M_p/m = 1836.152$ (M_p is the mass of the proton, M_d is the mass of the deuteron and m is the mass of the electron). Thus $V_p - V_f = 3.532\ kTe$ in the hydrogen plasma and $V_p - V_f = 3.878\ kTe$ in the deuterium plasma. This explains the observation by Inoue *et al* [103].

A detailed comparison of the negative ion density in the extraction region with the extracted beam current in hydrogen and deuterium operation has been done by Hamabe *et al* using a $35 \times 35\ cm^2$ and 18 cm deep arc discharge ion source [106]. These authors showed that the hydrogen and the deuterium negative ion density and beam current at 10 kW discharge power increased with gas pressure up to 15 mTorr, while the negative ion current density was always smaller for D^- than for H^-.

The larger co-extracted electron current is a severe difficulty for the D^- extraction because the power loading onto the extraction grid becomes unacceptable at higher acceleration and extraction voltages. A possible explanation for the larger co-extracted electron current in deuterium operation is the higher atomic fraction in a deuterium plasma compared to a hydrogen plasma, as shown by Péalat *et al* [102]. The mechanism which relates the higher atomic fraction to the larger co-extracted electron current is the following: due to the higher density of atoms, a larger destruction of the negative ions by associative detachment (reaction (3)) occurs, which generates additional electrons contributing to the electron current co-extracted with the negative ions. Péalat *et al* showed using CARS spectroscopy that the density of H_2 molecules in a 10 A discharge in a small magnetic multi-cusp plasma source was 71% of the density in the absence of discharge (i.e. density of the ideal gas at 540 K and 55 microbar), while the density of D_2 molecules was only 42% of the ideal gas at 540 K and 55 microbar, significantly lower than in H_2. The deficiency in molecules observed in deuterium compared to hydrogen leads to a lower negative ion production by DEA. According to Bacal *et al* [107] the deficiency in molecules in the D_2 discharge accompanied by a higher density of atomic deuterium explains the two times lower relative density of D^- observed in the operation of the

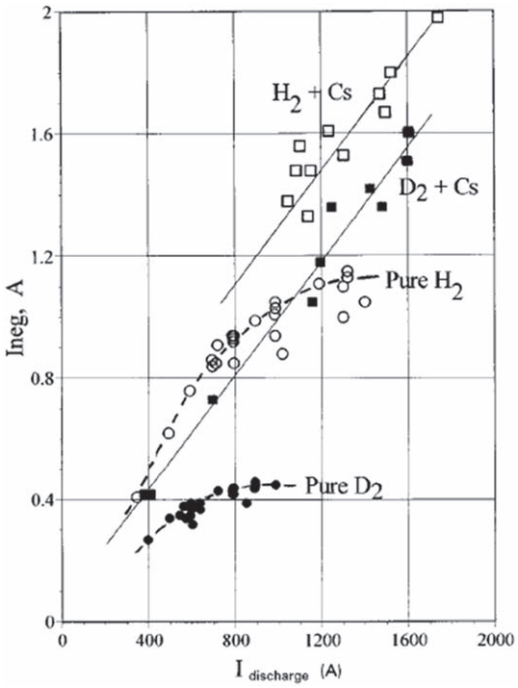

Figure 14. Negative ion current versus discharge current measured in the large negative ion source MANTIS by Jacquot *et al* [113] at source pressure of 5.6 mTorr. Reproduced from the article by C Jacquot *et al* 1996 *Rev. Sci. Instrum.* **67** 1036, figure 2, with the permission of AIP Publishing.

volume sources with D_2, namely $n^-/n_e = 0.06$ in deuterium versus $n^-/n_e = 0.12$ in hydrogen (see figure 2 in [108]).

Volume source operation with Cs seeding

The importance of surface negative ionization in a volume production type negative ion source was recognized in the US after Walther *et al* [108] showed that the Cs seeding to a hydrogen discharge resulted in a factor 16 increase in H^- current relative to the non-caesiated discharge for the same operating parameters. Operation of the source with the plasma electrode at optimum bias voltage was essential to obtain this result. The anode wall surface as well as the biased plasma electrode can produce H^-/D^- ions in this ion source geometry as suggested by Leung *et al* [109]. While Walther *et al* [108] worked on a tiny multicusp ion source of 2.5 cm radius and 5 cm long, Okumura *et al* [110] tested the effect of Cs injection into their source of 25 × 48 cm^2 area with 15 cm depth developed for a neutral beam heating system. They made the revolutionary step, that changed the evolution of the contemporary negative ion sources: by introducing caesium (Cs) vapor into a 46 kW arc power hydrogen discharge they extracted 7.8 A of H^- ion current.

Negative ion production in D_2 and H_2 was investigated by McAdams *et al* in a CW volume source at the Culham Laboratory and the results for both pure and caesiated source operation were reported by these authors [111]. For uncaesiated operation they showed how the performance depends on the cathode area by changing both filament number and diameter. This effect is attributed to the collection of ions from the plasma by the cathode structure. Through the use of caesium in the ion source the H^- and D^- current is enhanced by about a factor of two. Currents as high as 86 mA of H^- and 37.3 mA of D^- ions were extracted from a 16 mm diameter aperture.

Negative ion production in D_2 and H_2 was studied by Jacquot *et al* in the large multi-ampere source MANTIS with and without Cs addition into the discharge [112]. Figure 14 presents the negative ion current versus discharge current at a pressure of 5.6 mTorr, for both pure hydrogen and pure deuterium operation, as well as in both H_2 + Cs and D_2 + Cs operation. It is worth noting that operation in pure H_2 and pure D_2 exhibited saturation against discharge current increase, while operation with the caesium seeding presented a linear increase up to a larger value of the discharge current. While the ratio between the saturation level of the negative ion currents in H_2 and D_2 was about 3 for operation without Cs, the difference was significantly reduced by the caesium seeding. Negative ion current versus discharge current for full aperture extraction in figure 14 shows that the reduction of negative ion current was less than 20% by changing the gas from H_2 to D_2.

Bacal *et al* studied the effect of caesium seeding in the Camembert III plasma source when operated in H_2 and D_2 [107]. They measured the ratio of negative ion density to electron density, n^-/n_e in pure H_2 and pure D_2 at the center of the source extraction region using the photodetachment technique (see [38]). Figure 15 shows the dependence on the discharge current of the relative negative ion density in H_2 and D_2 with Cs seeding. The maximum value of n^-/n_e at the D_2 pressure of 1 mTorr was approximately 0.14. At the D_2 pressure of 3 mTorr the relative negative ion density was lower than that at 1 mTorr, and increased in proportion to the discharge current. These values were lower than those measured in H_2, where at 1 mTorr the maximum value of the relative negative ion density was approximately 0.25.

Surface sources

From 1980s, surface negative ionization processes have been commonly utilized to design efficient ion sources for a variety of negative ion species [114]. The surface negative hydrogen ion production appeared promising as the source for fusion plasma heating after the Novosibirsk group, Belchenko, Dimov and Dudnikov demonstrated that their caesiated surface-plasma source can produce 1 Amp level H^- ion beam [113]. Surface-plasma sources (SPS) developed by the Novosibirsk group produce very bright negative ion beams with the pulsed discharge current density exceeding 100 A cm^{-2}, which will be described in the following section. The high heat loading to the negative ion production surface of the original SPS, usually the anode of the magnetized discharge, was considered unfavorable for the stability of steady state operation for fusion plasma heating. Thus, the design to mitigate the power density onto the negatively biased electrode in a magnetic field free region of a multicusp

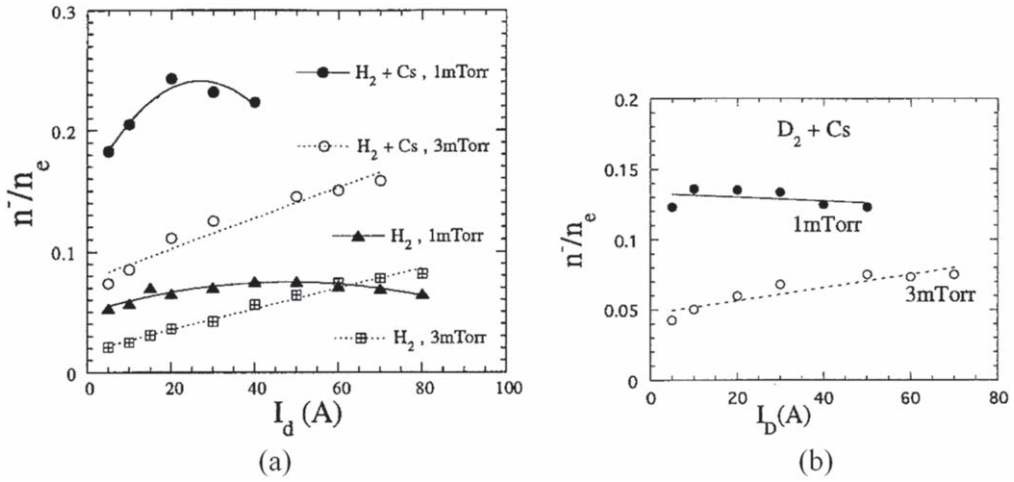

Figure 15. Comparison of the negative ion/electron density ratio between (a) H_2 and (b) D_2 operations. (Figure 3 in [109]: M Bacal *et al* 1996 *Rev. Sci. Instrum.* **67** (2) 1138.) Reproduced with the permission of AIP Publishing.

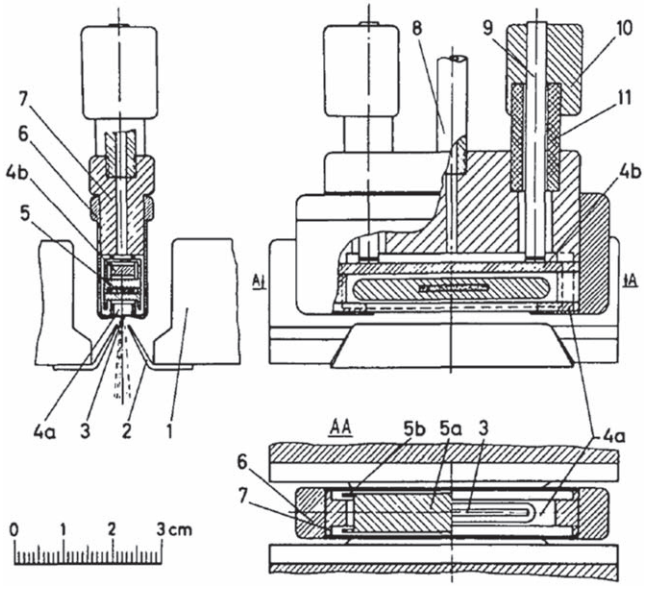

Figure 16. Schematic view of surface-plasma source: (1) Magnet; (2) extracting electrode; (3) emission slit; (4) anode ring; (5) cathode; (6) anode cover; (7) anode body; (8) hydrogen inlet pipe; (9) cathode inputs. (Figure 1 in [116]: Yu I Belchenko *et al* 1974 *Nucl. Fusion* **14** 113.)

plasma was employed so as to realize a stable emission of H^-/D^- from the electrode surface.

Magnetized plasma-surface source

The need of charge exchange injection into accelerators of hydrogen negative ion beams led to the development in Novosibirsk in the seventies of the last century by Dimov and his team of the surface-plasma sources (SPS) [113]. In his review Belchenko [115] defined the SPS as a source in which the negative ion production occurs on electrodes in contact with the gas discharge plasma, in contrast with 'pure surface' sources where ion production occurs due to reflection or desorption processes by pre-accelerated beams. Two versions of SPS were developed, namely the planotron, shown on figure 14, and the Penning type SPS [116]. In the planotron the discharge is established across a magnetic field of 1–2 kG inside a ring gap between a spool-like molybdenum cathode and a ring anode around the cathode. The duration of the discharge is 1–8 ms. During this time, the necessary density of hydrogen, about 10^{16} molecules cm^{-3} is established in the chamber and Cs, which is released from the cesium chromate pellets embeded into the cathode, is deposited on the electrodes. The voltage drop across the discharge is 100–150 V. When the positive ions from the discharge hit the caesium-coated cathode, an intense secondary emission of negative ions with a secondary negative ion emission coefficient higher than 10% sets in. Both reflection of positive hydrogen ions and sputtering of hydrogen atoms adsorbed on the cathode surface contribute to produce negative ions. The emitted negative ions are accelerated to the discharge plasma by the near-cathode potential drop. The negative ion current to the anode depends on the thickness of the anode plasma sheath since negative ions are destroyed in the gas-discharge plasma. The negative ions enter into the extraction region, where the beam is formed and accelerated to 20–30 keV through an emission slit in the anode across the magnetic field lines. As shown on figure 16, the pulsed SPS had small dimensions, while the source produced 0.88 A negative ion current through the 30 × 1 mm^2 emission slit.

Belchenko and Kupriyanov [116, 117] and Dudnikov [118] reported that the energy spectrum of the extracted H^- ions contained two groups: 80%–85% of these ions were produced on the cathode surface and the remaining 15%–20% were produced on the anode surface and in the near-anode plasma. According to Dudnikov [118] the production of the 'slow' ions of the second peak can be explained by the resonant change exchange of H^- ions with hydrogen atoms.

Dudnikov [119] reported in 1992 that the semiplanatron, a version of SPS, produced an H^- ion beam current of about 0.2 A. In 2002 he indicated [120] that the ion beam from an SPS has a current density j = 1–3 A cm^{-2}. In 2012 Dudnikov reported the generation of an H^- ion current of 40 A [121] and that the transverse H^- ion temperature from cesiated SPS

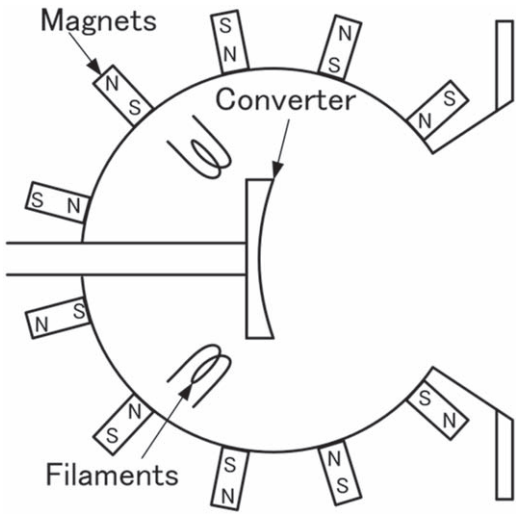

Figure 17. A schematic illustration of surface conversion source developed by Ehlers and Leung 1980 *Rev. Sci. Instrum.* **51** 721, [125] Reproduced with permission of AIP Publishing.

with noiseless discharges has been reduced to $T_i \sim 1$ eV with an emission current density $j \sim 1\ \mathrm{A\,cm^{-2}}$. A normalized rms emittance $\varepsilon_n \sim 0.2\pi$ mm mr was measured for an H^- ion beam with intensity $I \sim 0.1$ A extracted from a $0.6 \times 10\ \mathrm{mm^2}$ emission slit [118].

Efficient surface production of D^- was also achieved in a high-power density SPS: when the $2\ \mathrm{cm^2}$ surface-area cathode of the Penning source developed at Brookhaven National Laboratory was filled with a mixture of caesium chromate and titanium to supply Cs to the discharge, the source produced D^- current density as large as $25\ \mathrm{mA\,cm^{-2}}$ [122]. In his report [122], Prelec emphasized that the required discharge voltage to obtain the best D^- yield was around 400 V (420 V) as compared to the discharge voltage around 200–300 V for H^-. The lower velocity of D^- leaving from the cathode surface can be part of the reason why the D^- source needed higher discharge voltage. The results reported by Belchenko and Kupriyanov on their hollow cathode Penning source were more encouraging: the D^- current density was only about 15% lower than the H^- current density [116]. They attributed the possible reason for observing the lower D^- current density to be the negative ion loss in the dense discharge plasma.

Multicusp converter source

Highly intense discharges in magnetic fields generate electromagnetic noise which perturb the operation of the beam acceleration. Therefore, the high-power density of the SPS was considered to cause problems to the quasi-steady state operation of the neutral beam heating system for fusion plasmas. Much higher sputtering yields of deuterium ions compared to hydrogen ions against Mo cathode and the adsorbed Cs should also limit the life of the ion source under high power density operations of the discharge cathodes. Thus, the reduction of the power density was considered necessary to achieve a stable operation [123]. Surface conversion type ion sources utilizing the magnetic multicusp geometry to contain the negative ion production surface in the magnetic field-free region, were developed as the candidate source type for the negative-ion-based neutral beam heating system. The source geometry had the advantage that the suppression of the electron current co-extracted with the H^-/D^- ions appeared far much easier compared with volume sources in which electrons are extracted from the plasma with negative ions [124]. The prototype source developed by Ehlers and Leung had the dimensions of 20 cm diameter and 23 cm length and was equipped with a 6 cm high by 10 cm long copper electrode which worked as the converter [124]. This electrode called converter was immersed in H_2/D_2 plasma with the bias voltage several hundred volts negative with respect to the plasma. Negative ions of hydrogen and deuterium produced at the converter surface were 'self-extracted' across the sheath and passed through the plasma toward the extractor with the kinetic energy much larger than plasma electrons. The converter surface formed a concave geometry to focus the surface produced negative ion beam to the extractor as shown in figure 17.

When the source was operated without Cs, the signal intensity of the mass spectrometer facing the copper converter showed the energy spectrum of the surface produced H^- and D^- from atomic and molecular positive ions of the corresponding species: hydrogen and deuterium. The signal intensity of surface produced D^- was about 25% of that of the H^- signal for the copper converter. By directly introducing Cs into the discharge by heating two 10 cm long SAES Cs dispensers in front of the converter, the amount of surface produced H^- ions increased substantially, by a factor 100. The comparison between D^- and H^- was made with a Mo converter and the D^- production was found smaller than the H^- production by a factor of $\sqrt{2}$ [126].

The source size was enlarged to contain a concave 8×25 cm Mo converter to produce an H^- ion current exceeding 1 A [125]. The source operation with continuous feeding of Cs leads to breakdowns in the accelerator, since Cs vapor contaminates the accelerator system. A source design that did not require separate oven system was proposed by van Os *et al* with a solid Ba converter facing the edge of a magnetically suspended hydrogen isotope plasma and reported 4% conversion efficiency using hydrogen [127]. Heeren *et al* [128] used the experimental system of van Os *et al* to investigate the self-extracted D^- ion current from a $16\ \mathrm{cm^2}$ surface area Ba converter exposed to a magnetically suspended hydrogen isotope plasma and to compare the intensity with the self-extracted H^- ion current under the corresponding condition. They measured the effective conversion efficiency for D^- to be higher than that for H^-. The mentioned data on Ba converters [127, 128] may not be reliable because they could not be reproduced at another laboratory [129]. Therefore, Ba converters are not used further.

Lessons obtained from ion source development for fusion

We have introduced the change in ion source performance and/or beam forming system characteristics by replacing hydrogen by deuterium. It is now possible to discuss the

scenario for improving the negative ion source design for fusion plasma heating application. It is also possible to apply the obtained knowledge to deepen understanding, and to optimize the design for any kind of plasma source operated with deuterium.

Improvements of negative ion sources for fusion: current R and D status and future issues

In existing fusion test facilities the following two types of negative ion sources are utilized:

(1) The arc-filament discharge using Cs, as in the ion source operating in the Large Helical Device (LHD) [130] and JT-60U in Japan [131] and
(2) The RF driven negative ion source using Cs, as in the ion source planned for ITER [132, 133].

In the ion source operating with the arc-filament discharge the extraction region is separated from the discharge region. The intense arc discharge plasma is produced in the discharge region of the source with up to 400 kW arc power. The high temperature plasma is transported to the extraction region close to the PG passing through the magnetic filter field. The presence of the Cs vapor enhances the extracted D^- ion current density up to 190 A m^{-2} [130]. The RF driven negative ion source using Cs has been designed and tested at the Max-Planck-Institut für Plasmaphysik (IPP) in Garching, Germany [134, 135]. Since 2007 this RF driven source is the ITER reference source [132, 133]. The plasma is generated inductively ($f_{RF} = 1$ MHz, typical RF power: 70–100 kW) in the discharge region and then expands into an expansion region. The electrons are then cooled down by means of a magnetic filter field and reach the extraction region with an electron temperature of about 1 eV. In 2013 the ELISE test facility started operation. Its aim is to demonstrate long pulses (up to 1 h) at the power level of 80 kW/driver, at a filling pressure of about 2 mTorr. The most crucial factor limiting the source performance is a steady increase in the co-extracted electron current. The measures that counteract this steady increase are a long pulse Cs conditioning and modifying the filter field topology by adding the external permanent magnets [136].

The R&D required by the NBI design for DEMO and/or fusion reactors was discussed by Hemsworth *et al* [137] and Hemsworth and Boilson [138] Among the problems to be solved, those related to the negative ion sources are as follows:

1. Cesium. In order to attain the performance required for the ITER ion source it is currently estimated that it will be necessary to inject Cs into each source at a rate of 20 mg h^{-1}. Each of the three Cs ovens on each ITER injector will initially contain 40 g of Cs, which would allow the injectors to operate for more than 18 months: the expected length of an experimental campaign. If the same injection rate is required for the injectors on a continuously operating reactor, more than 1 kg of Cs will have been injected into each source every 6 years of operation, and as it has been found that most of the injected Cs remains in the ion source, this is likely to cause operational problems. Therefore, the source will have to be cleaned of Cs at some moment in the life of the reactor, or the entire ion source, and perhaps the extractor and accelerator, replaced. The latter requires a very expensive and difficult operation using remote means. Therefore, R&D is needed either to develop a technique for cleaning Cs from an ion source by some remote system, or the need to inject Cs must be reduced by about a factor 20 to allow operation for the reactor lifetime without cleaning the Cs out of the source, or an alternative to Cs developed.

2. Sputtering by back-streaming ions. Positive ions (D^+, D_2^+, Cs^+) created inside the accelerator, mainly via ionization of the residual gas by D^-, could be back-accelerated into the ion source and deposit a high power, about 1 MW, resulting in a high power density, on the ion source back-plate. One unwelcome consequence of the back-streaming ions is that they sputter material from the back-plate. Eventually the back-streaming ions will drill through the back-plate and reach the cooling water channel. On ITER this problem is avoided by having a thick molybdenum (Mo) layer on the back-plate. Due to the low sputtering yield of Mo a 1 mm thick layer of Mo will not be eroded away during the foreseen lifetime of ITER.

A second unwelcome consequence of the back-streaming ions is that some of the sputtered material is deposited on the PG and makes its work function higher, leading to a reduction of the negative ion production. When Cs is used to reduce the work function of the PG surface, the Cs layer is refreshed by the Cs injected into the ion source, but the PG deposited material due to sputtering may impose to increase the Cs injection rate to counteract its effect. These points together with the recently confirmed high ratio of co-extracted electron current to D^- current [130, 139, 140] are the topics being studied to realize the ITER NBI system.

Research to meet requirements for ITER NBI

The best solution for avoiding the Cs accumulation in the ion source is to realize a Cs-free source operation. Possibilities of Cs-free operation of negative ion source in a low pressure hydrogen discharge at ion source relevant parameters have been tested by Walther *et al al* [108] , Leung *et al* [141], and Bacal *et al* [142]. Walther *et al* [108] tested the operation of a small negative ion source by adding Xe, with the result that the H^- output increased by a factor 2.7 with respect to pure hydrogen operation at optimum pressure, while maintaining the same arc parameters. However, Leung *et al* [141] reported that the increase of the negative ion current when mixing xenon was observed only when the source was operated below the optimum hydrogen pressure, and therefore with lower H^- output. This optimum pressure was defined by maximizing the extracted H^- current. However, when the source was operated near optimum hydrogen pressure, adding Xe to the source did not improve the H^- current output. Bacal *et al* [142] confirmed and reinforced this negative result: they found that adding 0.3 mTorr of Xe to a hydrogen discharge at 3 mTorr enhanced the electron density by a factor 1.7, reduced the electron temperature by a factor 0.7 and reduced

the negative ion density by a factor 0.15. Leung *et al* [143] operated a multicusp ion source with a barium washer insert at the extraction aperture and found that the extractable H^- current is increased by a factor of 3 compared to a Cu insert when its bias potential is optimized.

Low work function materials, such as molybdenum doped with lanthanum, as well as different non-doped and boron-doped diamond samples were investigated by Kurutz *et al* [144] and Friedl *et al* [145] at ion source relevant plasma parameters. Cartry *et al* are investigating energy and angular distributions of surface produced hydrogen ions to search a material suitable for a PG of a negative ion source [146]. They reported that an overlayer of diamond may surface produce negative ions, but the stability against the plasma particle bombardment remained as an issue to be studied. This group has recently reported the result of the electride material that seemed stable against plasma ion bombardment while showing reasonable negative ionization efficiency [147]. The PG surface in Cs-free operation should withstand the deuterium plasma particle bombardment that transfers a momentum larger than the hydrogen plasma.

The larger mass of deuterons may also remove Cs from the PG more rapidly than protons. A molecular dynamic calculation result predicts that the difference in surface adsorption energies between the two isotopes is small [148]. But the larger mass of deuterons increases the removal of Cs, other adsorbates and Mo from the PG surface [149]. The data on sputtering yields [150], particle and energy reflection coefficients [65] for both hydrogen and deuterium are available to analyze the experimentally observed difference in negative ion current densities. Meanwhile, the mean ion energy in the source can be higher for deuterium. The bias voltage applied to the plasma electrode directly affects the incident ion energy, while Ikeda showed that the operation with a smaller co-extracted electron to negative ion current ratio required a more positive voltage (about 2.5 V) applied to their source PG and speculated on a higher plasma potential for the source operation with deuterium [151].

The ion source back-plate can show larger sputtering yield by deuterium compared to that by hydrogen due to back streaming positive ions. Ikeda *et al* found that the burn pattern at the back plate of their ion source changed in accordance with the shape of the extraction opening [151]. Kraus *et al* reported the Cu line spectrum emissions from their source probably due to plasma sputtering at the surface of their expansion chamber [152]. The sputtered materials from the back-plate and the expansion chamber walls can penetrate into the ion source plasma to cover the caesiated plasma grid, like tungsten from the filaments of arc discharge sources. This enhances Cs consumption rates forming Cs alloy that do not decompose to atomic Cs; this Cs does not reduce the work function of the PG [153]. The sputtered impurities can be also ionized in the plasma to be accelerated and sputter out Cs atoms on PG [154]. There are also positive effects due to sputtering: remove impurities embedded into the Cs surface and thus decrease the surface work function. Both positive and negative effects due to sputtering are expected to be more pronounced for deuterium than for hydrogen.

As reported by Hemsworth [155] the co-extracted electron currents are a major problem in the ion sources built for the neutral beam injectors of JET and ITER operating at a power as high at 800 MW. In these injectors the co-extracted electron current in D_2 was ten times larger than in H_2 [155]. Thus, Franzen *et al* [156] reported in 2011 that the minimal achieved co-extracted electron current was ten times higher than the extracted ion current in deuterium compared to hydrogen, for an extracted current density of 200 A m^{-2} for the ITER-size high-power RF negative ion source.

Fundamental processes causing a high coextracted electron current and negative ion current for a real size H^- ion source are being studied at National Institute for Fusion Science (NIFS) using the 35 cm wide, 70 cm long, 26 cm deep R&D Negative Ion Source (RNIS) with its highly integrated plasma diagnostics system [157–163]. Tsumori *et al* found that there exists a flow of negative ions near the PG which should determine the amount of extractable negative ion current from the PG apertures [157, 159]. The flow speed should be affected by the difference in mass between deuterium and hydrogen negative ions. The different negative ion current limitations for the surface produced negative ions induced by a virtual cathode [164] should also alter the transport of surface produced negative ions to the region where the extraction electric field penetrates into the plasma. This local plasma transport with the heavier mass of deuterons reduces the extractable amount of negative ion current while enlarges co-extracted electron current. Tsumori *et al* further tackled the problem of source operation with heavier mass ions using He, because charging deuterium into their ion source system will produce fusion neutrons. They found that the electron density and plasma potential of the plasma near the extractor increased as the mass of the discharge gas was increased [161]. These results suggest a larger electron density and a higher plasma potential for ion source operation with deuterium than with hydrogen. With the higher electron density the co-extracted electron current may increase, and an increase in intensity of the magnetic filter field should reduce the co-extracted electron current.

The RNIS device is a high temperature filament cathode driven arc discharge source, and has aspects different from the RF ion source as suggested by Fantz *et al* [162]. The operation of an arc discharge source with deuterium may increase the Cs consumption rate, as the Cs consumption rate of the arc discharge source is believed proportional to the tungsten cathode evaporation rate [163], and the tungsten loss from the cathode filament will be enhanced by the larger sputtering yield by deuterium ions. Thus, one has to note that an isotope effect like the change in Cs recycling may appear differently between an arc discharge source and an RF discharge source. Some maintenance requirements more complicated than the ones discussed in the past by Hemsworth *et al* [165] may be required for the neutral beam heating system. The RF source was chosen since 2007 as the reference source for ITER, which solves the Cs problem of enhanced sputtering yield of filaments by deuterium. The RF source is used in the test facility ELISE where Nocentini *et al* [166] challenge operation of long plasma pulses of up to 1 h.

As they extracted beams for 10 s in every 180 s interval, the extracted ion current tended to decrease slightly from one extraction pulse to the next, while the co-extracted electron currents increased substantially especially in deuterium operation. In certain extraction pulses the co-extracted electron current changed very dynamically and decreased during the beam-on phase. They attribute this in part to the influence of back-streaming positive ions which impact on the source back-plate and sputter Cs from its surface, therefore affecting the source condition [166]. Obviously the sputtering of Cs from the back-plate by the back-streaming deuterium ions is stronger than that due to hydrogen positive ions, which explains the observed isotope effect. More compilations of data with dependable diagnostics systems through expanding source operation scenarios [166] are necessary to define an operational mode that counteracts the instability caused by the isotope effect.

Applications to deuterium plasma source designs for neutron sources

Ion source development for D–D neutron production started in the 1950s [167] and by the end of 1970s deuterium ion beams with the intensity exceeding 100 mA were extracted from a duopigatron ion source and sent to the target for producing fusion neutrons [168]. The duopigatron ion source is a two-stage discharge between a hot cathode, an intermediate electrode and an anode. The plasma is guided by a carefully tailored axial magnetic field through a rather wide anode channel into a third chamber, at the end of which the electrons are reflected back towards the intermediate electrode.

From the old days of D^- beam development based on double charge exchange system, the source optimizations were attempted by using ion sources developed for hydrogen. Berkeley multi-cusp source [169] was developed and optimized as the positive hydrogen ion source for neutral beam heating of TFTR, and the performance was confirmed by operating the source with deuterium [170]. Namely, the source optimization using hydrogen gas without neutron production worked also for efficient deuterium operation.

Not only the fusion reaction produced radiations, but also various kinds of nuclear activations of the system by the primary radiation are the concerns for nuclear fusion research programs. Some components of a fusion reactor shall be irradiated by an intense neutron flux and the exposure to the neutron dose may deteriorate the material properties. The Fusion Material Irradiation Test (FMIT) Facility was proposed to confirm the material performance under continuous irradiation of fusion produced neutrons in a fusion based power system [170]. The deuteron ion sources developed for FMIT in early days were designed and operated mainly with hydrogen for tuning [171].

The International Fusion Material Irradiation Facility (IFMIF) was proposed based on accelerator and target technologies developed at FMIT. The project is now being propelled as the Broader Approach activities of ITER program [172]. The planned source for IFMIF was designed based upon the existing data base for hydrogen operation of ion sources [173]; the currently running project of the IFMIF Engineering Validation and Engineering Design Activity (EVEDA) employs an electron cyclotron resonance ion source for the D^+ beam production [174]. The initial system commissioning avoided activation of the components by extracting only protons [175], while the ion species compositions were compared between the source operation with hydrogen and that with deuterium [175]. The measured result indicated a slightly smaller monoatomic ion component, protons and deuterons, with some higher diatomic molecular ion component in the beam. The difference in ion species composition is attributed to the difference in cross sections in fundamental processes between the two hydrogen isotopes.

High brightness neutron source for neutron tomography [176] is being developed based on an advanced concept plasma source of the gas dynamic electron cyclotron resonance ion source [177]. Compact ion sources for neutron generators were further developed by Leung *et al* [178]. They produce deuterium beams for applications to boron neutron capture therapy (BNCT) [179] and radioisotope production for medical applications [33]. The targets for D–D neutron reaction can be also prepared based on deuteron plasma technology. The high-dose neutronsource described by Uhm and Lee [1] utilized the plasma ion implantation method described by Conrad *et al* [180]. Meanwhile, the laser induced plasma production technology can accelerate deuterons up to MeV energy range [181]. Further studies of deuterium plasma can make plasma focus [182] and z-pinch devices [183] as compact neutron sources of sufficient intensity.

Summary

This paper described the evolution of deuterium ion sources from double charge exchange sources towards volume sources, surface conversion sources and Cs added volume sources. Due to the larger atomic mass of deuterium compared to hydrogen different atomic and molecular reaction cross sections in plasma volume and also surface reaction rates for negative ion production and destruction have to be considered. The plasma transport toward the extractor is another process influenced by the ion mass; the larger mass of deuterium enlarges the ion Larmor radius requiring stronger filter magnetic fields. The deuterium positive ion transport across the magnetic field lines can increase the electron density in the vicinity of the extraction hole and thus the co-extracted electron current. The sputtering by the energetic positive deuterium ions of components exposed to the source plasma is enhanced. For the operation of a source designed for H^- ion extraction simply replacing the gas to deuterium, enhances positive ion transport from the driver region, and the increase in the sputtering yield should lead to a larger Cs consumption. Thus, the source design including the optimization of the filter field intensity as well as that of the

magnetic field structure is necessary to reduce Cs accumulation in the source to an allowable level.

It is not straightforward to realize a D^- ion source suitable for the future fusion machine based on reaction rates of volume and surface fundamental processes. Surface conditions and plasma parameters are correlated and can make the intensities of back-streaming ions and the final impurity production rate at the back plate unsuitable for the ion source operation. With the high maturity of the H^- ion source development, we may be ready to design a D^- source with suitable performance in negative ion intensity and co-extracted electron current. However, further optimization of the source design, for example of the back-plate material and structure, is necessary to achieve the smallest Cs accumulation in the source throughout the source operation life.

Acknowledgments

This work has been supported in part by Collaborative Research Program of National Institute of Fusion Science NIFS16KLER053, and in part by Japan Society for Promotion of Science KAKENHI No. 17H03512. We acknowledge enlightening discussions with Dr R S Hemsworth, Dr K N Leung and Dr R McAdams.

ORCID iDs

M Bacal https://orcid.org/0000-0003-2404-8052
M Wada https://orcid.org/0000-0001-9611-2004

References

[1] Uhm H S and Lee W M 1991 *J. Appl. Phys.* **69** 8056
[2] Fantz U *et al* 2018 *Fusion Eng. Des.* **136** 340
[3] Federici G, Biel W, Gilbert M R, Kemp R, Taylor N and Wenninger R 2017 *Nucl. Fusion* **57** 092002
[4] Simonin A *et al* 2015 *Nucl. Fusion* **55** 123020
[5] Matsuda S 2007 *Fusion Eng. Des.* **82** 435
[6] Leonov B V 2017 *Phys. At. Nucl.* **80** 1320
[7] Minaev V B *et al* 2017 *Nucl. Fusion* **57** 066047
[8] Santoso J, Manohoran R, Byrne S O and Corrr C S 2015 *Phys. Plasmas* **22** 093513
[9] Santoso J, Willett H V and Corr C S 2018 *Plasma Sources Sci. Technol.* **27** 10LT03
[10] Giruzzi G *et al* 2017 *Nucl. Fusion* **57** 085001
[11] Muroga T, Fukada S and Hayashi T 2019 *Fusion Sci. Technol.* **75** 559
[12] Berkner K H, Pyle R V and Sterns J W 1975 *Nucl. Fusion* **15** 249
[13] Fink J and Hamilton G W 1978 *IEEE Trans. Plasma Sci.* **PS-6** 41
[14] Heinemann B *et al* 2018 *Fusion Eng. Des.* **136** 569
[15] Wimmer C *et al* 2018 *Proc. 17th Int. Conf. on Ion Sources* 2011060001
[16] Kraus W, Wünderlich D, Fantz U, Heinemann B, Bonomo F and Riedl R 2018 *Rev. Sci. Instrum.* **89** 052102
[17] Leroy R 1991 Study of a hybrid multipolar source of hydrogen negative ions in view of extraction of an intense beam. Analysis of isotope effect using laser photodetachment techniques *PhD Thesis* University of Caen (in French)
[18] Leroy R, Bacal M, Berlemont P, Courteille C and Stern R A 1992 *Rev. Sci. Instrum.* **63** 2686
[19] Skinner D A, Bruneteau A M, Berlemont P, Courteille C, Leroy R and Bacal M 1993 *Phys. Rev.* E **48** 2122
[20] Fukumasa O, Mori S, Nakada N, Tauschi Y, Hamabe M, Tsumori K and Takeiri Y 2004 *Contrib. Plasma Phys.* **5–6** 516–22
[21] Friedl R, Cristoforo S and Fantz U 2018 *Proc. 17th Int. Conf. on Ion Sources: AIP Conf. Proc.* **2011** 050009
[22] Ogawa K *et al* 2017 *Nucl. Fusion* **57** 086012
[23] Heinemann B *et al* 2017 *New J. Phys.* **19** 015001
[24] Wünderlich D, Kraus W, Fröschle M, Riedl R, Fantz U and Heineman B 2017 *AIP Conf. Proc.* **1869** 030003
[25] Takeiri Y 2018 *IEEE Trans. Plasma Sci.* **46** 1411
[26] Chitarin A G *et al* 2018 *AIP Conf. Proc.* **2052** 030001
[27] Wünderlich D, Riedl R, Bonomo F, Mario I, Fantz U, Heinemann B, Kraus W and the NNBI team 2018 *AIP Conf. Proc.* **2052** 040001
[28] Holmes A J T, Dammertz G and Green T S 1985 *Rev. Sci. Instrum.* **56** 1697
[29] Green T S 1985 *Proc. 11th Symp. Fusion Eng. (Austin, TX)* pp 103–7
[30] McAdams R and Holmes A J T 1989 *Proc. SPIE* **1061** 514
[31] Fantz U *et al* 2017 *Nucl. Fusion* **57** 116007
[32] Bacal M, Sasao M, Wada M and McAdams R 2015 *AIP Conf. Proc.* **1655** 020001
[33] Leung K-N, Leung J K and Melville G 2018 *Appl. Radiat. Isot.* **137** 23
[34] Miller T J, Walsh C and Field T A 2017 Negative ions in space *Chem. Rev.* **117** 1765–95
[35] Chen J C Y and Peacher J L 1967 *Phys. Rev.* **163** 103
[36] Miller K A *et al* 2012 *Phys. Rev.* A **86** 032714
[37] Lykke K R, Murray K K and Lineberger W C 1991 *Phys. Rev.* A **43** 6104
[38] Bacal M 2000 *Rev. Sci. Instrum.* **71** 3981
[39] Peart B and Dolder K T 1973 *J. Phys. B: At. Mol. Phys.* **6** L359
[40] Mitchell J B A 1986 Dissociative recombination of molecular ions *Atomic Processes in Electron–Ion and Ion–Ion Collisions* ed F Brouillard (New York: Plenum) pp 185–222
[41] Mats Larson and Orel A E 2008 *Dissociative Recombination of Molecular Ions* (Cambridge: Cambridge University Press) p 201
[42] Hvostenko V I and Dukelskii V M 1958 *J. Exp. Theor. Phys.* **34** 1026
[43] Hvostenko V I and Dukelskii V M 1958 *Sov. Phys. JETP* **6** 657
[44] Schulz G J and Asundi R K 1967 *Phys. Rev.* **158** 25
[45] Demkov Y N 1965 *Phys. Lett.* **15** 235
[46] Schulz G J and Asundi R K 1965 *Phys. Rev. Lett.* **15** 946
[47] Rapp D, Sharp T E and Briglia D D 1965 *Phys. Rev. Lett.* **14** 533
[48] Allan M and Wong S F 1978 *Phys. Rev. Lett.* **41** 1791
[49] Orient O J and Chutjian A 1999 *Phys. Rev.* A **59** 4374
[50] Wadhera J M and Bardsley J N 1978 *Phys. Rev. Lett.* **41** 1795
[51] Bardsley J N and Wadhera J M 1979 *Phys. Rev.* A **20** 1398
[52] Gauyacq J P 1985 *J. Phys. B: At. Mol. Phys.* **18** 1859
[53] Wadhera J M 1979 *Appl. Phys. Lett.* **35** 917
[54] Celiberto R, Janev R K, Laricchiuta A, Capitelli M, Wadehra J M and Atems D E 2001 *At. Data Nucl. Data Tables* **77** 161–213
[55] Capitelli M *et al* 2006 *Nucl. Fusion* **46** S260
[56] Fabrikant I I, Wadehra J M and Xu Y 2002 *Phys. Scr.* **T96** 45
[57] Horacek J, Cizek M, Houfek K, Kolorenc P and Domcke W 2004 *Phys. Rev.* A **70** 052712
[58] Bruneteau A M, Courteille C, Leroy R and Bacal M 1996 *Rev. Sci. Instrum.* **67** 3827

[59] Courteille C, Bruneteau A M and Bacal M 1995 *Rev. Sci. Instrum.* **66** 2533
[60] Rasser B, van Wunnik J N M and Los J 1982 *Surf. Sci.* **118** 697
[61] Ernst-Vidalis M-L, Kamaratos M and Papageorgopoulos C 1987 *Surf. Sci.* **189/190** 276–84
[62] Blandin A, Nourtier A and Hone D 1976 *J. Phys.* **37** 369
[63] Kishinevskii M E 1975 *Zh. Tekh. Fiz.* **45** 1281
Kishinevskii M E 1975 *Sov. Phys.—Tech. Phys.* **20** 799 Engl. Transl.
[64] Hiskes J R, Karo A and Gardner M 1976 *J. Appl. Phys.* **47** 3888
[65] Eckstein W 2009 *IPP-Report* IPP 17/12 Max-Planck-Institut, Plasmaphysik
[66] Hiskes J R and Schneider P J 1981 *Phys. Rev.* B **23** 949
[67] Schneider P J, Berkner K H, Graham W G, Pyle R V and Sterns J W 1981 *Phys. Rev.* **23** 941
[68] Graham W G 1979 *Phys. Lett.* A **73** 186
[69] Yu M L 1978 *Phys. Rev. Lett.* **40** 574
[70] Pargellis A and Seidl M 1982 *Phys. Rev.* B **25** 4356
[71] Donnally B L, Clapp T, Sawyer W and Schulz M 1964 *Phys. Rev. Lett.* **12** 502
[72] D'yachkov B A and Zinenko V I 1968 *At. Energ. (USSR)* **24** 18(in Russian)
[73] D'yachkov B A, Zinenko V I and Pavlii M A 1972 *Sov. Phys.-Tech. Phys.* **16** 1868
[74] Martha Bacal and Reichelt W 1974 *Rev. Sci. Instrum.* **45** 769
[75] Bacal M, Truc A, Doucet H J, Lamain H and Chretien M 1974 *Nucl. Instrum. Methods* **114** 407
[76] Schlachter A S, Stalder K R and Stearns J W 1980 *Phys. Rev.* A **22** 2494
Schlachter A S 1977 *Proc. Symp. on the Production and Neutralization of Negative Ions and Beams, BNL-50727* (Brookhaven National Laboratory) p 11
[77] Vestergaard Hau L, Golovchenko J A and Burns M 1994 *Rev. Sci. Instrum.* **65** 3746
[78] Delaunay M *et al* 1980 *Proc. 2nd Int. Symp. on the Production and Neutralization of Negative Hydrogen Ions and Beams* (Brookhaven National Laboratory) p 255
[79] Geller R, Jacquot B, Jacquot C and Sermet P 1980 *Nucl. Instrum. Methods* **175** 261
[80] Bacal M, Doucet H J, Labaune G, Lamain H, Jacquot C and Verney S 1982 *Rev. Sci. Instrum.* **53** 159
[81] Osher J E, Gordon F G and Hamilton G W 1972 *Proc. 2nd Int. Ion Source Conf.* (Vienna)
[82] Grübler W, Schmelzbach P A, König V and Marmier P 1969 *Phys. Lett.* **29A** 440
[83] Hooper E B Jr, Anderson O A, Orzechowski T J and Poulsen P 1977 *Proc. Symp. on the Production and Neutralization of Negative Ions and Beams* (Brookhaven National Laboratory) BNL-50727*(Upton, New York)* p 163
Hooper E B Jr 1979 *IEEE Trans. Nucl. Sci.* **NS-26** 1287
[84] Semashko N N, Kusnetsov V V and Krylov A I 1977 *Proc. of the Symp. on the Production and Neutralization of Negative Ions and Beams* (Brookhaven National Laboratory) BNL-50727*(Upton, New York)* p 170
[85] Poulsen P and Hooper E B Jr 1979 *Proc. Symp. Eng. Problems Fusion Res.* vol 2, p 676
[86] Ehlers K W and Leung K N 1979 *Rev. Sci. Instrum.* **50** 1353
[87] Geller R, Jacquot C and Sermet P 1977 *Proc. Symp. on the Production and Neutralization of Negative Ions and Beams* (Brookhaven National Laboratory) p 173 BNL-50727
[88] Morgan T J 1977 *Proc. Symp. on the Production and Neutralization of Negative Ions and Beams* (Brookhaven National Laboratory) p 24 BNL-50727
[89] Hooper E B Jr, Poulsen P and Pincosy P A 1981 *J. Appl. Phys.* 52
1980 *Proc. of the Second Symp. on the Production and Neutralization of Negative Ions and Beams* (Brookhaven National Laboratory) p 247 BNL-51304
[90] Hooper E B, Poulsen P and Anderson O A 1982 *Nucl. Technol./Fusion* **2** 362
[91] Bacal M and Hamilton G W 1979 *Phys. Rev. Lett.* **42** 1538
[92] Bacal M, Nicolopoulou E and Doucet H J 1977 *Proc. Symp. on the Production and Neutralization of Negative Ions and Beams* p 26 BNL 50727
[93] Nicolopoulou E, Bacal M and Doucet H J 1977 *J. Phys.* **38** 1399
[94] Ehlers K W and Leung K N 1981 *Rev. Sci. Instrum.* **52** 1452
[95] Leung K N 1994 *Rev. Sci. Instrum.* **65** 1165
[96] Antipov G P, Elizarov L I, Martynov M I and Chesnokov V M 1990 Production and neutralization of negative ions and beams *AIP Conf. Proc.* **210** 184
[97] Leung K N and Ehlers K W 1984 *AIP Conf. Proc.* **111** 67
[98] Leung K N, Ehlers K W and Bacal M 1983 *Rev. Sci. Instrum.* **54** 56
[99] McAdams R and Holmes A J T 1989 *Proc. SPIE* **1061** 514
[100] Bacal M, Hatayama A and Peters J 2005 *IEEE Trans. Plasma Sci.* **33** 1845
[101] Livshits A I, ElBalghiti F and Bacal M 1994 *Plasma Sources Sci. Technol.* **3** 465
[102] Péalat M, Taran J P E, Bacal M and Hillion F 1985 *J. Chem. Phys.* **82** 4943
[103] Inoue T, Ackerman G D, Cooper W S, Hanada M, Kwan J W, Ohara Y, Okumura Y and Seki M 1990 *Rev. Sci. Instrum.* **61** 496
[104] Svarnas P, Breton J, Bacal M and Faulkner R 2007 *IEEE Trans. Plasma Sci.* **35** 1156
[105] Kuppel S, Matsushita D, Hatayama A and Bacal M 2011 *J. Appl. Phys.* **109** 013305
[106] Hamabe M, Oka Y, Osakabe M, Takeiri Y, Tsumori K and Kaneko O 2000 *Rev. Sci. Instrum.* **71** 1151
[107] Bacal M, Michaut C, Elizarov L I and Balghiti F E 1996 *Rev. Sci. Instrum.* **67** 1138
[108] Walther S R, Leung K N and Kunkel W B 1988 *J. Appl. Phys.* **64** 3424
[109] Leung K N, Walther S R and Kunkel W B 1989 *Phys. Rev. Lett.* **62** 764
[110] Okumura Y, Hanada M, Inoue T, Kojima H, Matsuda Y, Ohara Y, Seki M and Watanabe K 1990 *AIP Conf. Proc.* **210** 169
[111] McAdams R, King R F, Proudfoot G and Holmes A J T 1992 *AIP Conf. Proc.* **287** 353
[112] Jacquot C, Pamela J, Riz D and Belchenko Y 1996 *Rev. Sci. Instrum.* **67** 1036
[113] Belchenko Y I, Dimov G I and Dudnikov V G 1974 *Nucl. Fusion* **14** 113
[114] Middleton R and Adams C T 1974 *Nucl. Instrum. Methods* **118** 329
[115] Belchenko Y 1993 *Rev. Sci. Instrum.* **64** 1387
[116] Belchenko Y I and Kupriyanov A S 1994 *Rev. Sci. Instrum.* **65** 417
[117] Belchenko Y I and Kupriyanov A S 1994 *Rev. Sci. Instrum.* **65** 1170
[118] Dudnikov V G 2017 *AIP Conf. Proc.* **1869** 030044
[119] Dudnikov V G 1992 *Rev. Sci. Instrum.* **63** 2660
[120] Dudnikov V G 2002 *Rev. Sci. Instrum.* **73** 992
[121] Dudnikov V G 2012 *Rev. Sci. Instrum.* **83** 02A708
[122] Prelec K 1977 *Nucl. Instrum. Methods* **144** 413
[123] Cooper W S 1984 *AIP Conf. Proc.* **111** 605
[124] Ehlers K W and Leung K N 1980 *Rev. Sci. Instrum.* **51** 721
[125] Lietzke A F, Ehlers K W and Leung K N 1984 *AIP Conf. Proc.* **111** 344

[126] Ehlers K W and Leung K N 1983 *Proc. 2nd Int. Symp. on Production and Neutralization of Negative Hydrogen Ions and Beams* pp 198 BNL 51304
[127] van Os C F A, Heeren R M A and van Amersfoort P W 1987 *Appl. Phys. Lett.* **51** 1495
[128] Heeren R M A, Ciric D, Yagura S, Hopman H J and Kleyn A W 1992 *Nucl. Instrum. Methods* B **69** 389
[129] Kwan J W 2019 private communication
[130] Ikeda K *et al* 2019 *Nucl. Fusion* **59** 076009
[131] Kojima A *et al* 2017 *Fusion Eng. Des.* **123** 236
[132] Mimo A, Wimmer C, Wunderlich D and Fantz U 2018 *AIP Conf. Proc.* **2052** 040009
[133] Wünderlich D, Kraus W, Fröschle M, Riedl R, Fantz U and Heinemann B 2017 *AIP Conf. Proc.* **1869** 030003
[134] Speth E *et al* 2006 *Nucl. Fusion* **46** S220
[135] Staebler A *et al* 2009 *Fusion Eng. Des.* **84** 265
[136] Fantz U, Schiesko L and Wünderlich D 2014 *Plasma Sources Sci. Technol.* **23** 044002
[137] Hemsworth R S *et al* 2017 *New J. Phys.* **19** 025005
[138] Hemsworth R S and Boilson D 2017 *AIP Conf. Proc.* **1869** 060001
[139] Ikeda K *et al* 2018 *AIP Conf. Proc.* **2011** 060002
[140] Ikeda K *et al* 2019 *Rev. Sci. Instrum.* **90** 113322
[141] Leung K N, Hauck C A, Kunkel W B and Walther S R 1989 *Rev. Sci. Instrum.* **60** 531
[142] Bacal M, Bruneteau A M, Deniset C, Elizarov L I, Sube F and Tontegode A Y 2000 *Rev. Sci. Instrum.* **71** 1082
[143] Leung K N, van Os C F A and Kunkel W B 1991 *Appl. Phys. Lett.* **58** 1467
[144] Kurutz U, Friedl R and Fantz U 2017 *Plasma Phys. Control. Fusion* **59** 075008
[145] Friedl R, Cristofaro S and Fantz U 2018 *AIP Conf. Proc.* **2011** 050009
[146] Cartry G *et al* 2017 *New J. Phys.* **19** 025010
[147] Sasao M, Moussaoui R, Kogut D, Ellis J, Cartry G, Wada M, Tsumori K and Hosono H 2018 *Appl. Phys. Express* **11** 066201
[148] Rutigliano M, Palma A and Sanna N 2018 *Plasma Sources Sci. Technol.* **27** 115006
[149] Wada M, Doi K and Kenmotsu T 2017 *AIP Conf. Proc.* 1869020003
[150] Behrisch R and Eckstein W (ed) 2007 *Sputtering by Particle Bombardment* (New York: Springer)
Matsunami N *et al* 1980 *Inst. Plasma Phys.* Report IPPJ-AM14 Nagoya Univ.
[151] Ikeda K, Kisaki M, Nakano H, Nagaoka K, Osakabe M, Kamio S, Tsumori K, Geng S and Takeiri Y 2017 *AIP Conf. Proc.* **1869** 050004
[152] Kraus W, Schiesko L, Wimmer C, Fantz U and Heinemann B 2017 *AIP Conf. Proc.* **1869** 030006
[153] Krylov A, Boilson D, Fantz U, Hemsworth R S, Provitina O, Pontremoli S and Zaniol B 2006 *Nucl. Fusion* **46** S324
[154] Wada M 2018 *Rev. Sci. Instrum.* **89** 052103
[155] Hemsworth R 2018 private communication
[156] Franzen P *et al* 2011 *Nucl. Fusion* **51** 073035
[157] Tsumori K *et al* 2012 *Rev. Sci. Instrum.* **83** 02B116
[158] Tsumori K *et al* 2016 *Rev. Sci. Instrum.* **87** 02B936
[159] Tsumori K and Wada M 2017 *New J. Phys.* **19** 045002
[160] McAdams R, King D B, Holmes A J T and Surrey E 2012 *Rev. Sci. Instrum.* **83** 02B109
[161] Tsumori K *et al* 2018 *AIP Conf. Proc.* **2052** 040015
[162] Fantz U, Falter H D, Franzen P, Speth E, Hemsworth R, Boilson D and Krylov A 2006 *Rev. Sci. Instrum.* **77** 03A516
[163] Takeiri Y *et al* 2013 *AIP Conf. Proc.* **1515** 139
[164] Hemsworth R S, Boilson B, De Esch H P L, Krylov A, Massmann P and Svensson L 2006 *Nucl. Fusion* **46** S239
[165] Nocentini R, Fantz U, Froeschle M, Heinemann B, Kraus W, Riedl R and Wuenderlich D 2017 *Fusion Eng. Des.* **123** 263
[166] Wunderlich D, Riedl R, Fantz U, Heinemann B, Kraus W and NNBI team 2018 *Plasma Phys. Control. Fusion* **60** 085007
[167] Blosmsjo E and von Dardel D F 1955 *Appl. Sci. Res.* **4** 49
[168] Bacon F M and Riedel A A 1979 *IEEE Trans. Nucl. Sci.* **NS-26** 1505
[169] Vella M C, Cooper W S, Pincosy P A, Pyle R V, Weber P D and Wells R D 1988 *Rev. Sci. Instrum.* **59** 2357
[170] Hagan J W, Opperman E K and Trego A L 1984 *J. Nucl. Mater.* **123** I958
[171] Armstrong D D, Meyer E A, Rutkowski H L and Schneider J D 1979 *IEEE Trans. Nucl. Sci.* **NS-26** 3009
[172] Okumura Y 2013 *Fusion Sci. Technol.* **64** 86
[173] Kinsho M, Sugimoto M, Seki M, Oguri H and Okumura Y 2000 *Rev. Sci. Instrum.* **71** 963
[174] Delferriere O, De Menezes D, Gobin R, Harrault F and Tuske O 2008 *Rev. Sci. Instrum.* **79** 02B723
[175] Shinto K *et al* 2016 *Rev. Sci. Instrum.* **87** 02A727
[176] Golubev S, Skalyga V, Izotov I and Sidorov A 2017 *J. Instrum.* **12** T02003
[177] Skalyga V *et al* 2016 *Rev. Sci. Instrum.* **87** 02A716
[178] Leung K N 2000 *Rev. Sci. Instrum.* **71** 1064
[179] Leung K N 2012 *Neutron Capture Therapy: Principles and Applications* (New York: Springer) p 55
[180] Conrad J R, Radtke J L, Dodd R A, Worzala F J and Tran N C 1987 *J. Appl. Phys.* **62** 4591
[181] Sunahara A, Asahina T, Nagatomo. H, Hanayama R, Mima3 K, Tanaka H, Kato Y and Nakai S 2019 *Plasma Phys. Control. Fusion* **61** 025002
[182] Jain J *et al* 2017 *AIP Adv.* **7** 085121
[183] Klir D *et al* 2018 *New J. Phys.* **20** 053064